ON IDENTIFYING FREQUENCIES AND DAMPING IN SUBCRITICAL FLUTTER TESTING

John C. Houbolt

Aeronautical Research Associates of Princeton, Inc.

SUMMARY

A review is given of various procedures that might be used in evaluating system response characteristics as involved in subcritical flight and wind-tunnel flutter testing of aircraft. Emphasis is given to the means for eliminating or minimizing the contamination effects produced by an unknown noise in the input. Results of a newly developed procedure for identifying modal frequency and damping values, and a possible way for making a detailed evaluation of system parameters, are also given.

INTRODUCTION

The purpose of this report is to give a review of various procedures that might be used in evaluating system response characteristics as involved in subcritical flight and wind tunnel flutter testing of aircraft. The aim in such testing is generally to evaluate modal damping and frequencies as a function of flight speed. In some cases, studies aim to identify the system parameters in greater detail, such as identifying the coefficients of a modelled differential equation of motion.

In practical subcritical flutter testing three main problems arise: (1) there usually is an unknown noise input, such as that due to turbulence, and this contamination makes the system response evaluation very difficult, uncertain, or impossible; (2) time for a test run must often be kept short, such as less than 10 seconds (for example, to achieve a given speed the airplane may have to be put in a shallow dive and the interval of time over which test conditions are reasonably constant is therefore limited), shortness of records in turn aggravates the noise problem; and (3) an underlying desire is to be able to perform rapid analyses of the records so that the tests may proceed almost immediately to the next test run. The procedures presented herein represent various attempts to cope with these problems, with emphasis being given to means for minimizing or obviating the noise problem.

Much of the material in this report is covered in reference 1, which contains a number of references to other work; no other reference is therefore cited. Some new findings are included.

RELEVANT EQUATIONS

Let the general governing differential equation for response for the airplane subcritical flutter system be given by

$$D_1 y = D_2 P \tag{1}$$

where D_1 and D_2 are differential operators, and y is the response to the forcing function P. The force P may be a prescribed force, as obtained from a shaker, or it may be some unknown quantity, such as due to atmospheric turbulence, and these forces may be acting singly or in combination.

If the input force is a Dirac function $\delta(0)$ at $t = 0$, equation (1) defines the impulse response function h as follows

$$D_1 h = D_2 \delta(0) \tag{2}$$

For a unit sinusoidal input, $P = e^{i\omega t}$, and with

$$y = He^{i\omega t}$$

equation (1) yields the frequency response function

$$H(\omega) = A(\omega) + iB(\omega) \tag{3}$$

according to the equation

$$(\Delta_1 + i\Delta_2)(A + iB) = N_1 + iN_2 \tag{4}$$

where Δ_1, N_1 and Δ_2, N_2 are the real and imaginary parts that are associated with the operators D_1 and D_2. The A component of H is symmetrical with respect to the frequency ω, the B component is antisymmetrical.

The h and H functions are related by the Fourier transform pair

$$H = \int_0^\infty he^{-i\omega t}\, dt \tag{5}$$

$$h = \frac{1}{2\pi} \int_{-\infty}^{\infty} He^{i\omega t}\, d\omega \tag{6}$$

By the superposition theorem, the solution of equation (1), for any general forcing function P, is given by

$$y = \int_{-\infty}^{\infty} P(\tau)h(t - \tau)d\tau \tag{7}$$

The Fourier transform of this equation is

$$F_y(\omega) = H(\omega)F_P(\omega) \tag{8}$$

from which H follows as

$$H = \frac{F_y}{F_P} \tag{9}$$

Equation (8) also leads to the well-known spectral result

$$\phi_y = |H|^2\phi_P \tag{10}$$

If P is equal to $P + Q$, where P is a known force, and Q is an unknown "noise" force, equation (8) would appear

$$F_y = H(F_P + F_Q)$$

The multiplication through the complex conjugate $\bar{F}_P$ leads in turn to the spectral equation

$$\phi_{Py} = H(\phi_P + \phi_{PQ}) \tag{11}$$

where ϕ_{Py} is the cross spectrum between P and y, ϕ_P is the spectrum of P, and ϕ_{PQ} is the cross spectrum between P and Q. If P and Q are uncorrelated, $\phi_{PQ} = 0$, and thus equation (11) yields the important cross-spectrum equation

$$H = \frac{\phi_{Py}}{\phi_P} \tag{12}$$

which appears as a completely noise-free result.

Reference 1 gives some significant special solutions to equation (1), as follows.

I:

$$D_1 R_h = D_2 h(-t) \tag{13}$$

where

$$R_h = \int_{-\infty}^{\infty} h(\tau)h(t + \tau)d\tau \tag{14}$$

Thus, the autocorrelation function of h is the response of the system to a force input of $h(-t)$.

II:

$$D_1 y_n = D_2 Q_n \tag{15}$$

where Q_n is white noise. For this situation, it can be shown that $R_{y_n} = R_h$; thus, the correlation function of the response to white noise is the same as the autocorrelation function of the impulse function h .

III:

$$D_1 R_{Py} = D_2 R_P \tag{16}$$

Thus, if the autocorrelation function of an input P is applied to the system as an input force, the response is the cross-correlation function between P and the response y due to P .

CLASSIFICATION OF THE SWEPT SINE FUNCTION

Forcing inputs are achieved by several means, such as inertial shakers or aerodynamic vane exciters, explosive charges, stick raps, and the natural turbulence of the atmosphere. Of all these means, vane exciters or shakers are most commonly used. For the forcing function, the swept sine wave has become a popular choice, mainly because it covers a sizable frequency band in a short period of time and because the spectral content of this function resembles white noise. The rate of sweep and total duration are prime variables; with some tests the sweep rate is fast, in others the rate is quite slow. For discussion and testing purposes, it appears desirable to make a classification of the duration of sweep. The rate of change of frequency depends of course on the frequency range covered and the duration required to make the sweep. For the testing of most aircraft systems, however,

it appears that classification can be based mainly on duration alone. The following classification is suggested:

1) Fast sweep - one made with a duration of about 5 to 10 seconds

2) Moderate sweep - duration of around 1 minute

3) Slow sweep - duration of around 5 minutes

Each of these sweeps has certain advantages and certain deficiencies, depending on the application. The slow sweep is the best for minimizing noise, but the drawback is long testing and record analysis times. In many instances, though, test conditions dictate the use of fast sweeps.

DAMPING AND FREQUENCY EVALUATION FOR THE IDEAL CASE

Figure 1 indicates three basic ways for evaluating the damping and frequency of a mode. It is assumed that a test has been made, such as through application of a swept sine wave forcing function, and that the response has been analyzed to obtain H (equation (9)), which yields B and A, $C^2 = |H|^2 = A^2 + B^2$, and h (equation (6)). The situation depicted by this figure is ideal; that is, there is no noise present in the input and only a single mode is involved. The top sketch depicts the transfer loci or admittance plot involving A and B. The resonant frequency f_o is identified at the point where there is the greatest rate of change of arc length with respect to a change in the frequency. The damping ratio $\frac{\beta}{\beta_{cr}}$ is given by the equation shown. In the second scheme involving $C^2 = A^2 + B^2$ plotted against f, the modal frequency is identified by the location of the peak, the damping by the width at 1/2 power. In the third scheme, involving damped unforced motion after some excitation, frequency is identified by the period T, damping by the log decrement equation.

Note, the offhand appearance of a peak (second sketch of figure 1) may at first cause a misinterpretation of damping. In figure 2, for example, the peaks on the right visually seem to indicate more damping than the peaks on the left; all peaks on the same line have the same damping, however, as measured in terms of percent of critical damping. Likewise, the three peaks on the right of the middle sketch have the same damping, even though the shortest peak seems to suggest a larger damping than the tallest peak.

Other means for deducing frequency and damping involve curve-fitting procedures, such as fitting the experimentally derived frequency response function H, or fitting the impulse response function h, and then deducing the roots from the fitted curves.

When modes are close together, or when noise is present in the input, the techniques of figure 1 break down. It is towards handling the situation of the presence of a number of modes and the contamination due to an unknown noise source that the remainder of this report is devoted.

THE USE OF EXCITERS AND TRANSDUCERS IN COMBINATION

It is odd that little in general has been done in using transducers in pairs as a way of helping to solve the closely spaced mode situation, particularly in separating the symmetrical and antisymmetrical modes which have frequencies close together. Figure 3 serves as a reminder of what practices should be followed in general. With one shaker, say on the right, the use of only the signal from point 1 makes it very difficult to distinguish the symmetric mode from the antisymmetric mode. The addition of the signals from point 1 and point 2, however, identifies the symmetric mode and virtually eliminates the antisymmetric mode. The subtraction of the signals, on the other hand, identifies the antisymmetric mode to the exclusion of the symmetric mode. This subtraction scheme also provides for good rejection of symmetric excitation due to noise.

For two shakers, one on the left and one on the right, use of y_1 or $y_1 + y_2$ for in-phase excitation gives symmetric mode isolation. If the two shakers are 180° out of phase, y_1 or $y_1 - y_2$ gives good antisymmetric mode isolation. Again, in this case, $y_1 - y_2$ also gives good rejection of symmetric excitation due to noise.

The use of two pick-ups in a different chordwise position, such as at points 3 and 4, also should be considered as a way of helping to isolate closely spaced modes; the idea here is that excitation of different modes appears in a different relative sense according to the closeness to the nodal lines.

Figure 4 depicts results obtained for a three-mode system, with two symmetric modes of 3 Hz and 10 Hz and one antisymmetric mode of 9.8 Hz; thus, the antisymmetric mode had a frequency only 2 percent different from one of the symmetric modes. With one shaker, a swept sine wave excitation, and only one pick-up, the deduced results for A, B, C^2, B vs A, and h, indicate that only two modes are present, one around 3 Hz and one around 10 Hz.

Figure 5 applies to one-shaker excitation of the same system, but the signals from a right and a left transducer are subtracted. The marked change in the results is a clear indication that two modes are present near 10 Hz. For figure 6, the situation is the same as for figure 5, except that a strong symmetric excitation due to noise is also present. The results, in spite of the noise, gives a tip-off that there are two closely spaced modes around 10 Hz. Thus, with one shaker operation, the technique of adding the signals from two opposite transducers and of subtracting the signals and comparing the deduced results appears as a good way to establish whether two modes with frequencies close together - one symmetric, one antisymmetric - are present. Two shakers, first used symmetrically then antisymmetrically, provide an even better way to isolate symmetric and antisymmetric modes.

INITIAL SEQUENCE OF DATA ANALYSIS

Some of the first data analysis checks that should be made are often overlooked in a testing sequence. A review of certain initial steps that should be performed is thus considered worthwhile.

It is assumed that tests are being made with a swept sine force input. The first analysis that should be made is to make an attempt to identify modal frequencies roughly, to classify the modes as to whether they are symmetrical or antisymmetrical, and to see if the apparent modes can be identified with ground vibration modes. Suggested first steps are as follows:

1) Combine signals as indicated in the previous section.

2) Scan the combined time history signals and look for "bursts" in the response; the object here is to obtain a rough idea of the modal frequencies and to establish whether the mode is symmetric or antisymmetric and whether primarily bending or torsion.

3) From the signals, establish raw H values (equation (9)) and in turn h values (equation (6)). Clear h, according to the cleared h procedure discussed subsequently, transform back to first improved H, and form $C^2 = |H|^2 = A^2 + B^2$. Examine the C^2 function to obtain a second check on the modal frequencies (verify those established by scanning the time history signals, pick up others that may have been missed) and to obtain a first estimation of modal damping where possible.

4) From the appearance of the C^2 functions, an assessment of the noise problem can be made, and a judgment can be

rendered as to what type procedures should be used subsequently to minimize the noise problem.

Essentially, the idea behind these steps is to do something quite simple at first so as to obtain a quick insight as to what the frequencies might be and to obtain a quick appraisal of the severity and nature of the noise problem.

TECHNIQUES FOR MINIMIZING OR ELIMINATING INPUT NOISE EFFECTS

Use of Both Input and Output Information

Six schemes for coping with the problem of having noise in the input are presented in brief fashion in this section. (See reference 1 for more detail.) It is assumed that one or more shakers are used to drive the system, such as by a swept sine wave, and that an unknown excitation noise force, such as due to buffeting or atmospheric turbulence, is also present.

Clearing h.- Figure 7 is typical of the results that are obtained for H and h, by means of equations (9) and (6), when a large input noise is present along with the swept sine wave excitation. One way to eliminate much of the noise contamination is simply to clear or erase the results for h beyond a point where useful information no longer seems to appear, such as point a in figure 7, and then to transform this truncated h back to H (eq. (5)). Example results are given in figure 8. The remarkable improvement that is obtained for the A and B values by doing this simple expedient is seen.

Weighting h.- Another technique is shown in figure 9. Here the raw h is weighted by an exponential function; the weighted result is then transformed back to give refined A and B values. This technique, as with figure 8, reduces noise effects greatly. With this weighting technique, a correction to the deduced values of damping must be made to correct for the apparent damping that is added by the weighting function used.

Use of cross correlation between input and output.- Figure 10(a) applies to the raw results as obtained by use of equation (9). By contrast, the results shown in figure 10(b) were obtained by use of equation (12), which involves the cross spectrum between the measured output and the known shaker force input. This cross-correlation technique is seen to give a marked improvement in the deduced A and B values. In general, the longer the record, the better is the noise minimization by this technique.

Peak shifting.- Figure 11 is used to describe the peak shifting technique for eliminating noise effects. The top sketch depicts the swept sine wave input force, the bottom sketch the noise-contaminated response. First, select a peak such as a . Then select peak b and shift the entire record so as to make peak b fall on peak a . Next, take peak c and shift the record to make peak c fall on a . Do this for a number of peaks in succession, and then add all the results to form a composite input force designated by

$$P_T = \sum P_n$$

The output response is handled in the same way, but using the same shifts as used for the input; the composite response is designated as

$$y_T = \sum y_n$$

Now deduce H from P_T and y_T , using equation (9). The concept in this technique is that a single short record may be used and that the shifting and adding operations cause the meaningful or intelligent part of the record to be enhanced, amplified, or reinforced, while the noise level remains the same (or the signal-to-noise ratio increases). Figure 12 gives results obtained in a particular case where only 19 shifts were made. In the main frequency range of interest, around 10 Hz, it is seen that practically noise-free results are obtained. A feature of the peak shifting scheme is that it is possible to concentrate on various frequency ranges even with the use of a single record. For example, in figure 11, two "bursts" in the output response are noted, suggesting two frequencies of possible concern. To concentrate on the lower frequency, peaks in the vicinity of peak a are shifted to fall at peak a ; to concentrate on the higher frequency, peaks in the vicinity of peak p are shifted.

Ensemble averaging.- In ensemble averaging, the concept is to deduce, by repeat runs, a number of raw estimates for the function h , and then to add all the raw functions together. The idea is that this averaging-type operation will "average out" noise effects and leave only the meaningful signal. Example results, involving an ensemble average of 20 raw functions, are shown in figure 13. It is seen that virtually noise-free results are obtained. This is one of the best schemes for eliminating noise, but the main drawback is that it requires making a number of repeat runs.

Sweep over limited frequency band.- Figure 14 is given as a help to describe a limited sweep approach. Suppose that test sweeps are made to cover the range of 3 Hz to 25 Hz in 10 seconds, and consider that the analysis of the results indicate some modal

information in the range of 10 Hz but that the results are too noisy to be interpreted with confidence. A good way to improve the situation is to sweep over only the frequency range of concern, say, in this case, from 8 Hz to 12 Hz in the 10 seconds of sweep time. Generally, a vast improvement in the deduced results will be noted. The disadvantage, of course, is the problem of resetting the sweep range and of having to make another run.

Use of Output Information Only

There are at least two ways to derive system response characteristics by consideration of the output response alone. The procedures apply in general whether the response is due to a forced swept excitation with an unknown noise input or whether the response is due to noise excitation alone.

One procedure involves the establishment of the auto-correlation function R_y of the output response. Each side or half of this symmetric function has characteristics of the h function. The Fourier transform of R_y is the spectrum ϕ_y of the response. Examination of this spectrum gives an indication of the frequency and damping of the system modes. Ensemble averaging of the R_y functions is found to be a powerful way to minimize noise by this approach, reference 1. Other ways to use the R_y function and minimize noise will be indicated in the subsequent section.

A second procedure for deriving system response characteristics using response information alone is the formation of the "randomdec" signature. The essentials of one type of construction for this approach are shown in figure 15. It can be reasoned that the sum of all the individual signals should form a pure signal which resembles or has characteristics of the h function. Damping and frequency follow from the resulting summed signal. A main difficulty of the approach is that the summation must often involve hundreds of functions before converged values of the sum are achieved. Another difficulty is in identifying closely spaced modes.

SUCCESSIVE CORRELATIONS OF CORRELATION RESULTS - A PROMISING SOLUTION TO THE NOISE PROBLEM

Under a contract effort for AFFTC/AFSC, Edwards AFB, the author has developed additional techniques for treating the noise problem - techniques which appear remarkable and in a way unbelievable. This section summarizes some of the results

obtained. The procedures involved are quite versatile and represent subsequent manipulations for improving the quality of the results that are obtained by most all the procedures described earlier in this report. Two figures are presented first as a way to describe the procedures involved. In figure 16, the top sketch refers to autocorrelation of the raw h function (see eq. (14)) that has been deduced by any of the procedures discussed previously, or it refers to the autocorrelation R_y, obtained by considering only the response (due to noise alone, due to a swept sine wave alone, or due to these forcing functions acting in combination). Note, the raw h should always be cleared as discussed in connection with figures 7 and 8. Likewise, if the autocorrelation function is used, the "noisy" tails (the tail portions on either side which appear to be due to noise only) should be erased. Then the following steps are performed:

1) Make R_1 one-sided; call it r_1

2) Form R_2, the autocorrelation of r_1

3) Form ϕ_2, the Fourier transform of R_2; look at this function for improvement (reduction in noise content) and for mode identification

4) Go back to R_2

5) Make R_2 one-sided; call it r_2

6) Repeat these steps as often as necessary until the spectrum ϕ_n appears without distortion due to noise.

In the application of these steps, the following will occur:

1) The modes which show up with low power will first disappear (means for recovering these modes will be discussed subsequently).

2) The mode with the next lowest power (actually a combination of power and damping) will then disappear, and so on, until finally only one mode remains.

3) With each iteration, the results become more and more noise-free.

4) Sometimes, depending on modal power and damping and on mode closeness, noise-free results will occur with perhaps two or three modes still remaining.

5) The reading of the frequency and damping of these remaining modes, by the second scheme of figure 1, will be

an accurate indication of the frequency and damping of these modes.

Figure 17 illustrates a companion type manipulation. In this case, the correlation functions are kept in their two-sided form; thus, a correlation function of a correlation function is found, in succession. In this case, the following should be observed.

1) The modes with the lowest power lose more and more power with each iteration and finally disappear.

2) The peaks become more and more spiked; damping is lost, but frequency is more and more sharply pinpointed.

Although the theory is not given here, it should be noted that the consequences of the two types of manipulation described can be explained on a theoretical basis.

Means for recovering any lost mode are as follows. Go back to the original spectrum type function ϕ_1. In figure 16, peak a would probably have remained to the end. But, suppose it was desired to identify the mode inicated by b more precisely. In this case, simply erase the ϕ_1 function above frequency ω_2 and below ω_1 (in this case, erasing above ω_2 is all that is required); application of the steps described earlier will then bring out mode b in a pure form.

Figure 18 shows results as obtained by the one-sided procedure, using h as established from a raw or contaminated H. The experiment involved use of an analog simulation of a system; excitation was by means of a linear swept sine wave, and an unknown random noise. In part (a), we see frequencies around 3 Hz and 10 Hz, but the precise location and damping cannot be established. In part (b), which represents the first iteration, mode 1 has just about disappeared, and the rest of the function is much more noise-free. By 5 iterations, mode 2 has become very pure; damping and frequency are nearly precisely the values set in the analog set up (in this case, $f_o = 10$ Hz, $\frac{\beta}{\beta_{cr}} = 0.05$).

Figure 19 gives results using the response only, and its autocorrelation, for the same run of figure 18. The raw spectrum indicates the two modes in the vicinity of 3 Hz and 10 Hz. By three iterations, the 10 Hz mode is identified purely.

In figure 20, end results are shown for convergence to the mode near 3 Hz. In this case, strain response rather than acceleration response was used, and convergence went automatically to the lowest mode (no spectrum erasing had to be performed).

Note, displacement or strain emphasizes the lower modes, while acceleration response, due to the ω^2 weighting, emphasizes the higher modes.

Figure 21 serves to show the remarkable power of the procedure to regenerate correct frequency and damping information when severe truncations in the frequency plane are made. Figure 21(a) is the original spectrum of h obtained for a one-mode system and without noise in the input. The shaded areas were then erased; after several iterations, starting with this truncated spectrum, the spectrum as indicated by figure 21(b) was found. Frequency and damping of the mode is still intact. The experiment was repeated, truncating figure 21(a) to the severe form shown by figure 21(c); here truncation is within the half-power limits. After several iterations, the results shown in figure 21(d) were obtained. Damping and frequency are still the same as the original, even though the only information used was that given by figure 21(c).

Figure 22 shows results that were obtained with a system having frequencies of 9 and 10 Hz, both with $\frac{\beta}{\beta_{cr}} = 0.05$. Figure 22(a) represents the raw or contaminated spectrum of h . After several iterations by the one-sided approach, the result shown in figure 22(b) was obtained; the frequency and damping are in excellent agreement with the model values. Figure 22(c) represents the spectrum as obtained by considering the response only. Figure 22(d) is the result obtained by the one-sided approach after information beyond f_c was erased; this erasing was done to bring out the lower mode. The damping and frequency indicated by figure 22(d) for this mode is in good agreement with the correct values, even though the information contained in peak 1 was all that was used. Figure 22(e) is the result obtained by applying the two-sided approach to the R_y function; the tendency to form sharp spikes is shown by this sketch.

Figure 23 applies to a system having modes fairly close together as follows:

Mode	f,Hz	β/β_{cr}
1	8	0.05
2	9	0.05
3	10	0.02

Figure 23(a) is the raw spectrum of h . If no erasing is made, application of the sequence of steps would result in the 10 Hz mode coming out in pure form. Clearing beyond f_a yielded the result shown by figure 23(b) by the one-sided approach; clearing

before f_a and beyond f_b yielded the result shown by figure 23(c). Damping and frequencies for both modes are very good. Thus, both lower modes were extracted, in spite of the closeness of another mode having a much lower value of damping.

SYSTEM PARAMETER IDENTIFICATION - POSSIBILITIES OF A NEW APPROACH

A number of different schemes have been studied as means for obtaining a more detailed identification of system parameters. These schemes generally fall under three categories:

1) Curve fitting of the frequency response function

2) Fitting of time plane information, such as the h function

3) Difference-equation approaches in which the coefficients of a difference-equation model are evaluated, from which system roots may in turn be extracted

Collocation procedures are sometimes used for the curve-fitting operations but, more generally, the approaches are based on the use of least-squares concepts. Some of the system identification approaches are reviewed and developed in reference 1 and the references contained therein. Thus, they will not be discussed further herein. Instead, the notions of a possible new approach will be outlined.

A commonly used concept in subcritical flutter testing of an aircraft is to make a plot of damping g versus V, figure 24. The basic idea is to establish the trend of the damping curves and to extrapolate forward to estimate the flight speed at which the damping vanishes (or reduces to some stipulated lower level). This procedure is reasonably satisfactory for a mild approach to the critical flutter speed, curve a, but is quite treacherous when an explosive flutter situation is encountered, curve b, for in this situation the damping can deteriorate very quickly with only a small increase in speed. A way to obviate this problem is sought. Reference 1 suggests one possible procedure. The idea is to derive the coefficients of the assumed governing differential equation model and to watch how these coefficients vary with air speed. Figure 25, taken from reference 1, depicts results for the situation of a mild approach to flutter. The nature of the extrapolation is known by analytical considerations; for example, the coefficients a_3, a_2, a_1, and a_0 are known to vary in a quadratic manner. Extrapolation to higher speeds seems straightforward. With the extrapolated coefficients, system

roots for higher speeds may be evaluated, from which an estimate of the critical flutter speed may be made. Figure 26 shows the behavior of the coefficients for a system which has explosive flutter characteristics. In figure 25 the variation of the coefficients appears gradual, while in figure 26 two of the coefficients, specifically a_2 and a_3, are changing quite markedly with V. This rapid, but not abrupt, change in the coefficients with speed appears as a tip-off that the situation may be of the explosive flutter variety.

We now combine the thoughts associated with figures 25 and 26 with the procedures discussed in the previous section. Suppose that the procedures outlined in the previous section stand the test of more extensive study and that the procedures indeed are reliable in establishing the frequencies and damping of the various modes of the system under study. With the frequencies and damping established, the governing differential equation can then be formed. As an example, consider that three modes are identified; roots may then be written as

$$p_1 = \left(\frac{g_1}{2} + i\right)\omega_1$$

$$\bar{p}_1 = \left(\frac{g_1}{2} - i\right)\omega_1$$

$$p_2 = \left(\frac{g_2}{2} + i\right)\omega_2$$

$$\bar{p}_2 = \left(\frac{g_2}{2} - i\right)\omega_2$$

$$p_3 = \left(\frac{g_3}{2} + i\right)\omega_3$$

$$\bar{p}_3 = \left(\frac{g_3}{2} - i\right)\omega_3$$

where $g_n = 2\left(\frac{\beta}{\beta_{cr}}\right)_n$. From these roots, the governing differential equation follows as

$$(p - p_1)(p - \bar{p}_1)(p - p_2)(p - \bar{p}_2)(p - p_3)(p - \bar{p}_3) = 0$$

Expansion of this equation yields the characteristic equation

$$p^6 + a_5p^5 + a_4p^4 + a_3p^3 + a_2p^2 + a_1p + a_o = 0$$

which in turn defines the coefficients a_n of the governing differential equation. In accordance with figures 25 and 26, we watch how these coefficients vary with air speed.

We note that curve fitting in the frequency plane or time plane, or any other evaluation of coefficients through use of least-squares procedures, is precluded in this suggested approach. The success depends simply on the reliable estimation of the mode frequency and damping values.

CONCLUDING REMARKS

Which one of the procedures outlined herein for minimizing noise effects is the best? No specific choice can really be made. A systematic study is needed to try each procedure in a number of different applications and circumstances. The choice of which is best will undoubtedly depend on the situation encountered. Nevertheless, some comment about certain features or drawbacks of the procedures can be made.

The procedure of clearing the impulse response function h (rectangular truncation) should always be used, no matter how h has been derived. The exponential weighting of the raw h is not suggested in general, since the cleared h process serves just about as well. The use of the cross-spectrum approach is considered one of the best but generally is more applicable for the longer sweep times. The peak shifting technique is very attractive but of course requires the intermediate step of shifting and summing the record portions. Ensemble averaging is perhaps the best but is probably precluded in most instances because of the necessity for making a number of repeat runs. Randomdec is not advocated unless a swept sine wave forming function is used (with a noise input alone, too many terms are required in the summation in general). Where response information only is available, the autocorrelation approach (or equivalently, the spectrum of the response) should, of course, be used. In this approach, care should be taken to erase the "noisy" tails of the correlation function, as mentioned in the body of the report. Also, in this approach it is likely that fairly long record lengths are available; this works to the favor of the approach because, on the whole, the longer the record the better the results (as in the general rule for most all approaches).

As a general comment, while there is a science to the procedures for minimizing the noise problem, there is also an art in their applications. Depending on the circumstances and the type

of analysis equipment available, little "tricks" can be inserted at appropriate places to gain an improvement in the end results.

REFERENCE

1. Houbolt, John C.: Subcritical Flutter Testing and System Identification. NASA CR-132480, August 1974.

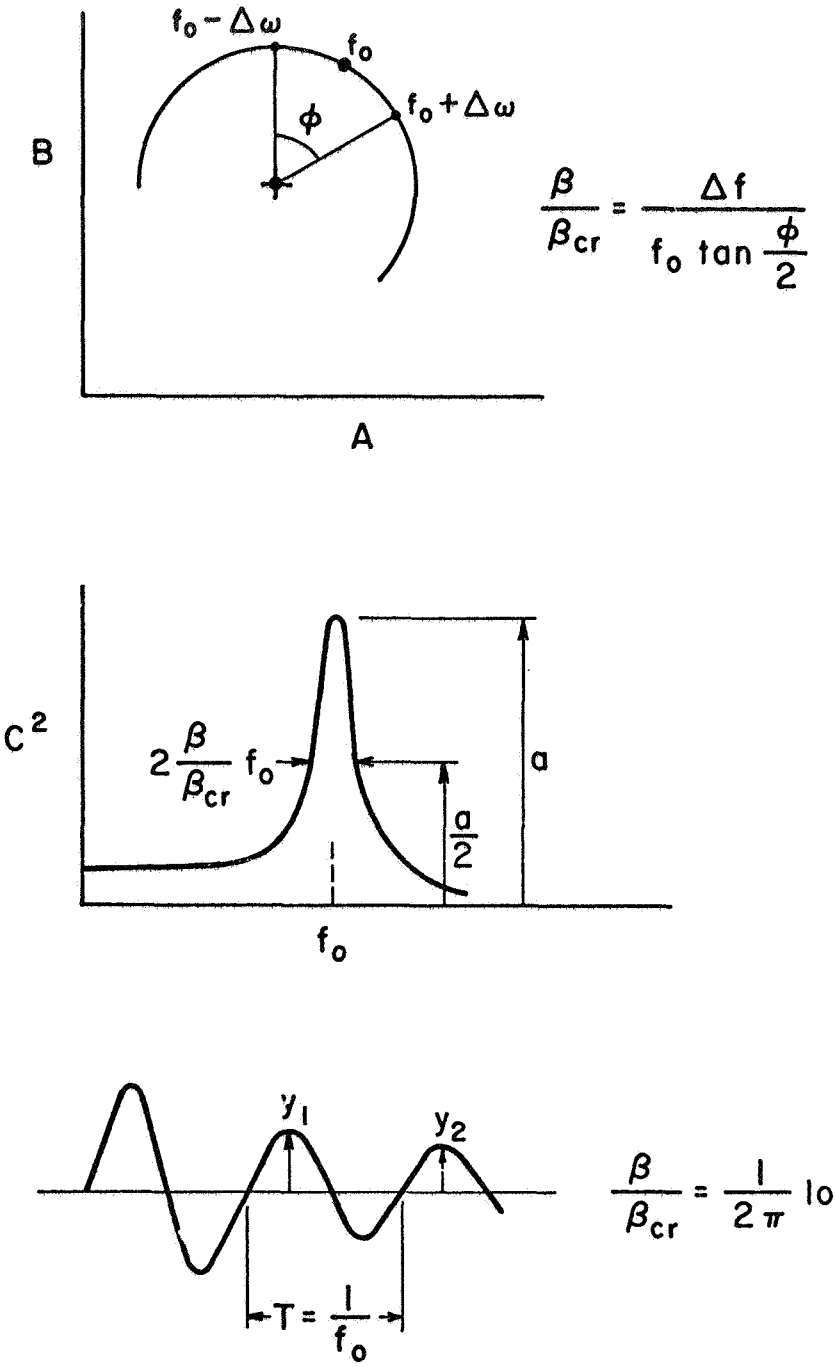

Figure 1.- Three basic ways for estimating modal frequencies and damping.

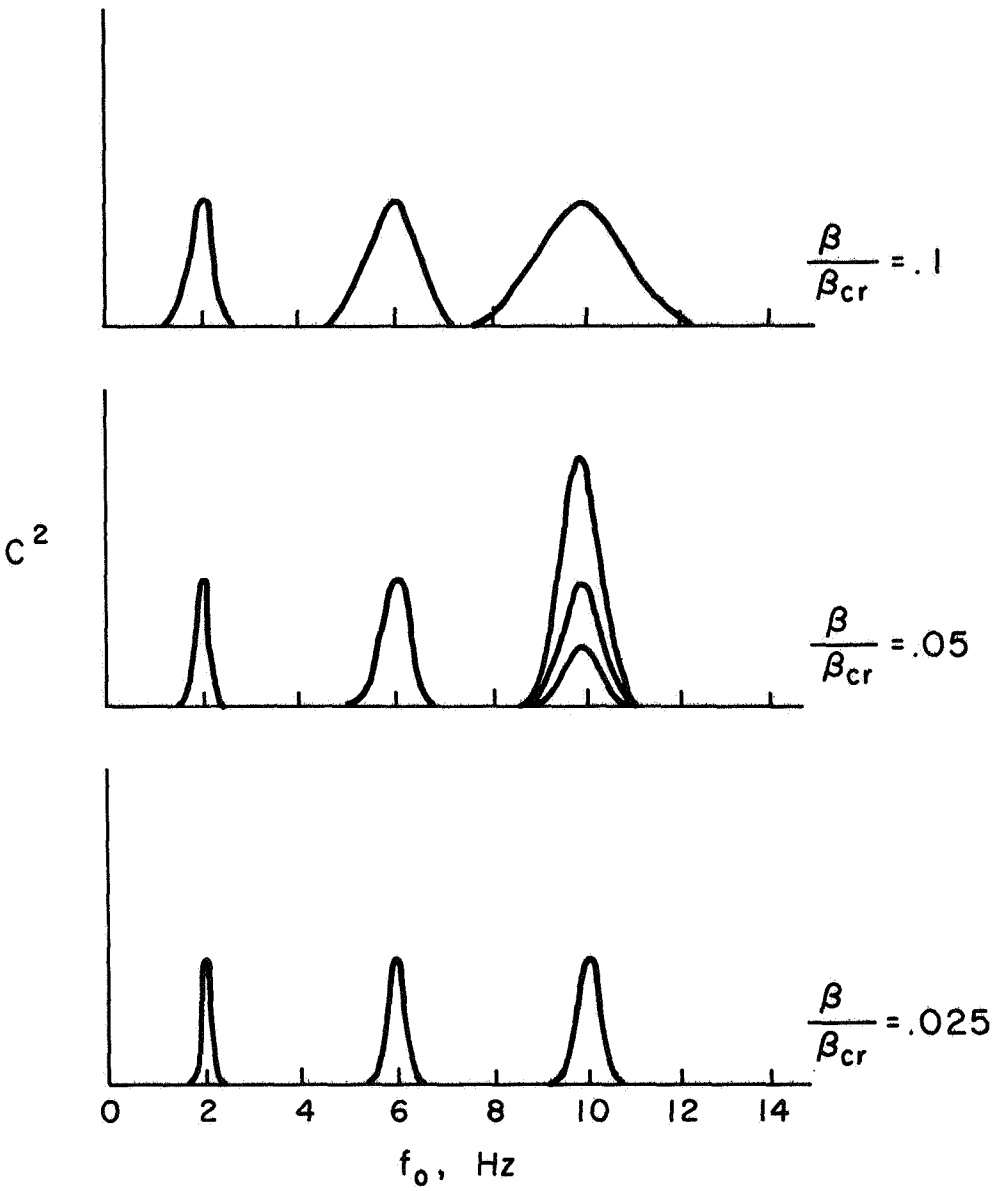

Figure 2.- Appearance of resonance peaks of different damping.

One Shaker:

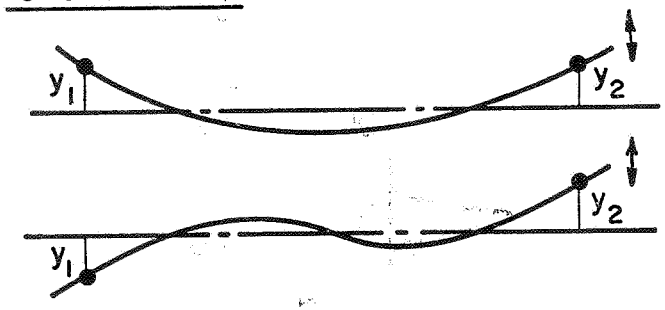

$y_1 + y_2$

$y_1 - y_2$ — good elimination of symmetric excitation due to noise

Two Shakers:

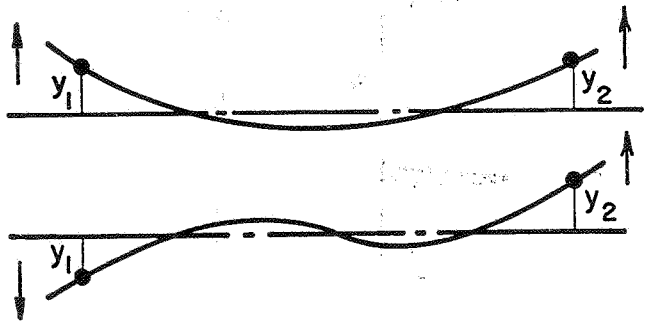

y_1 or $y_1 + y_2$

y_1 or $y_1 - y_2$, for better elimination of symmetric excitation due to noise

also for y_3 & y_4

Figure 3.- Combining response signals to identify symmetric and antisymmetric modes.

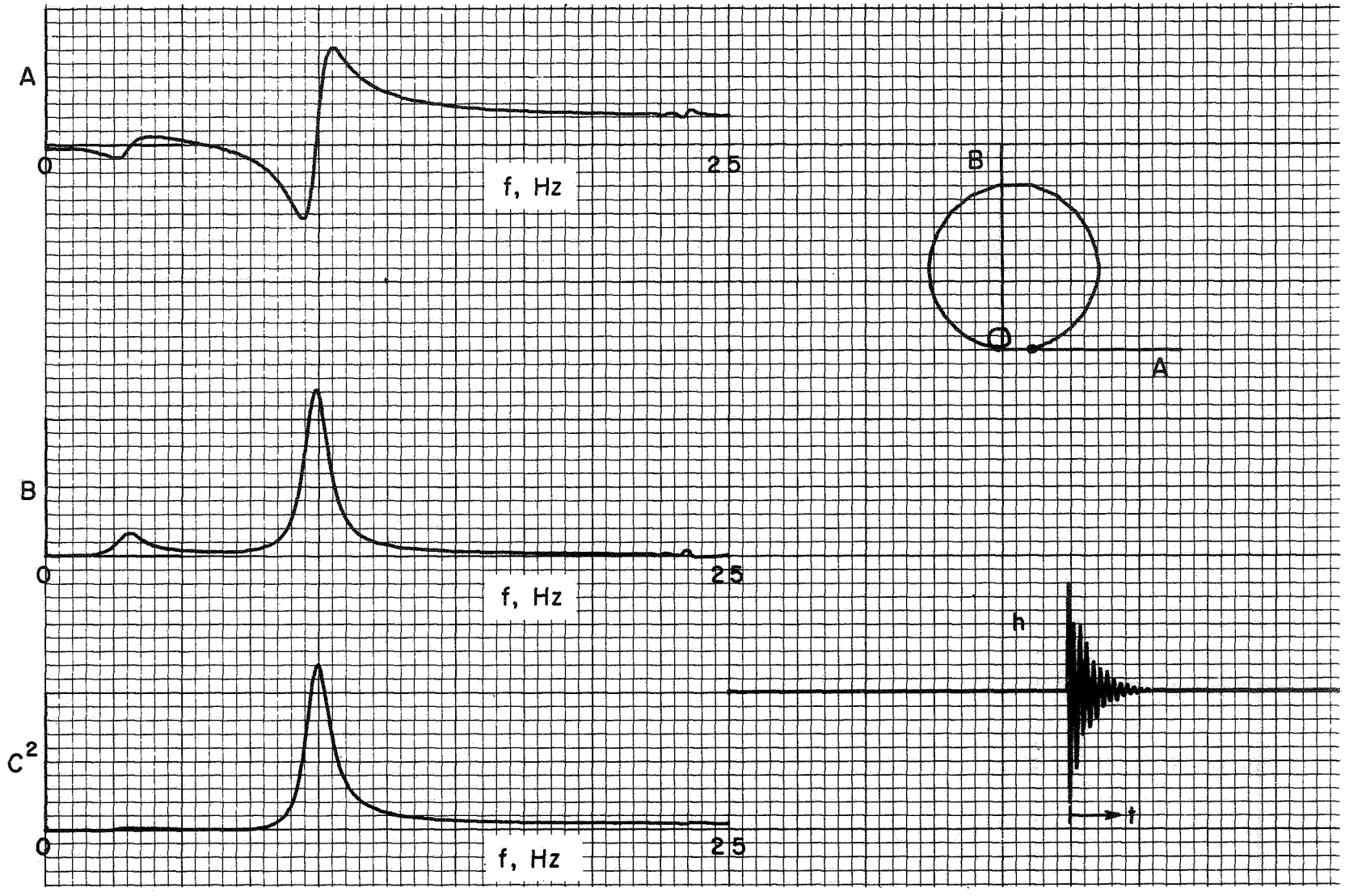

Figure 4.- Response results for three-mode system, one shaker, adding tip responses.

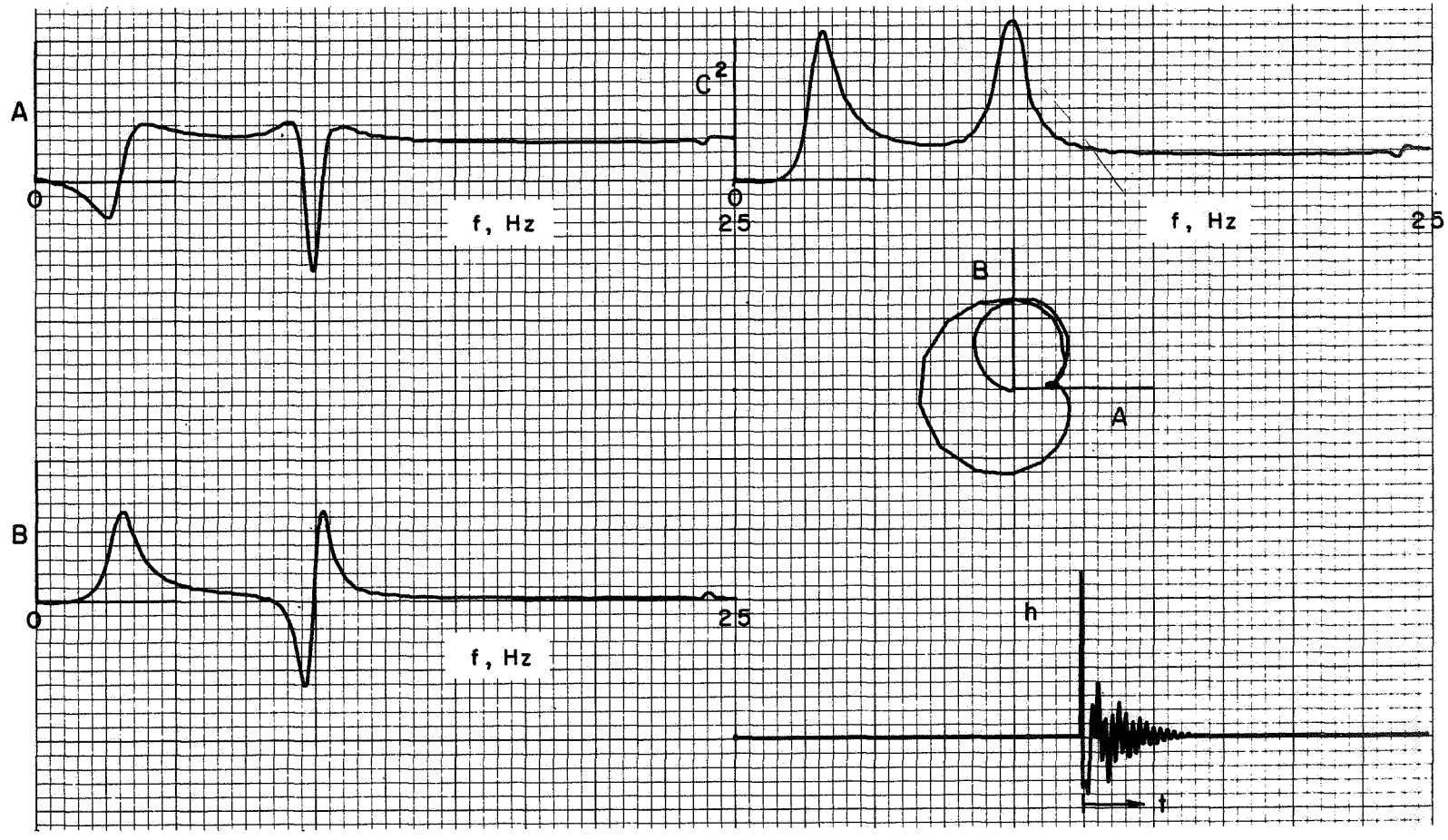

Figure 5.- Response results for three-mode system of figure 3, one shaker, subtracting tip responses.

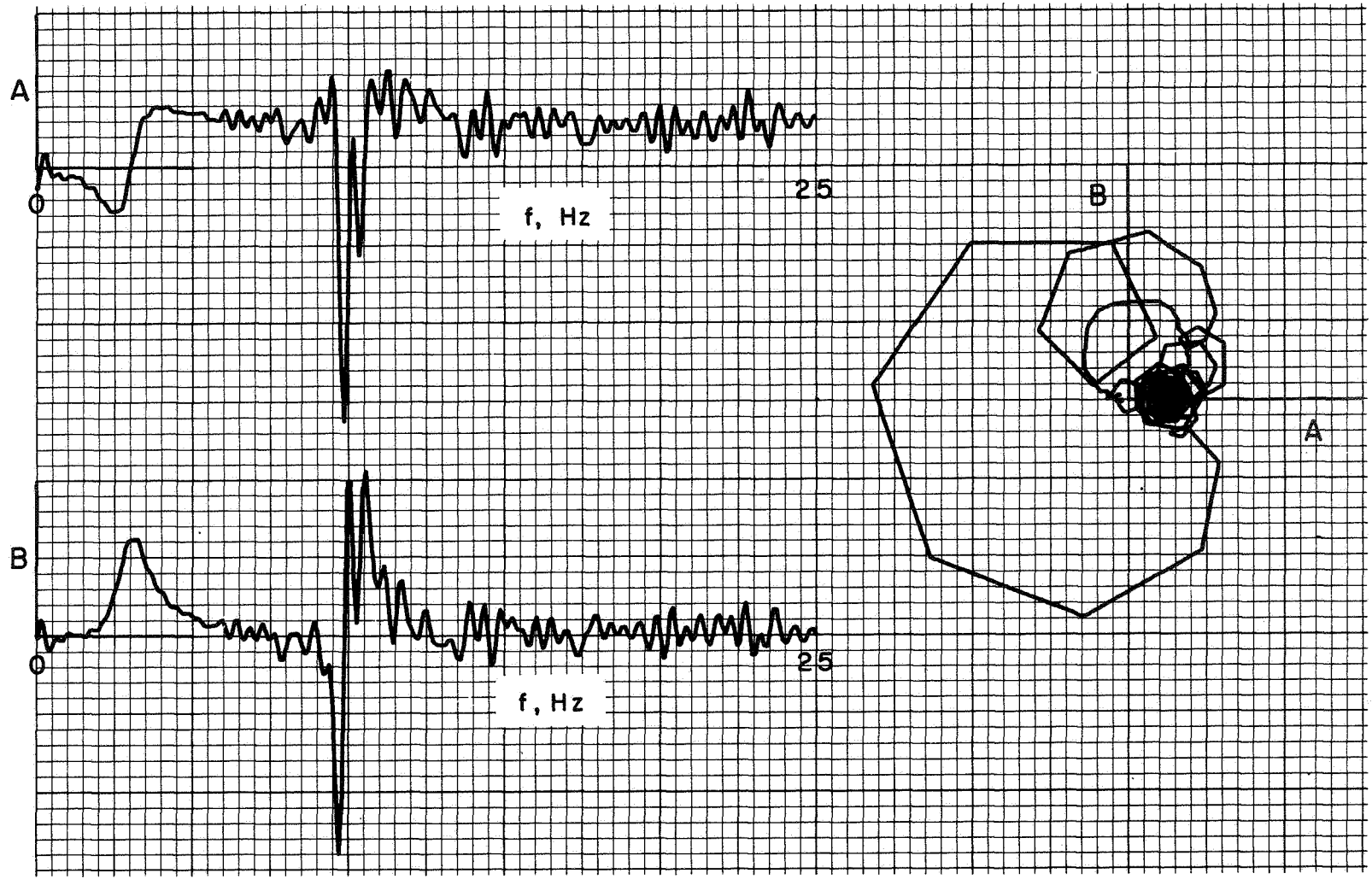

Figure 6.- The situation of figure 5 with noise in the input.

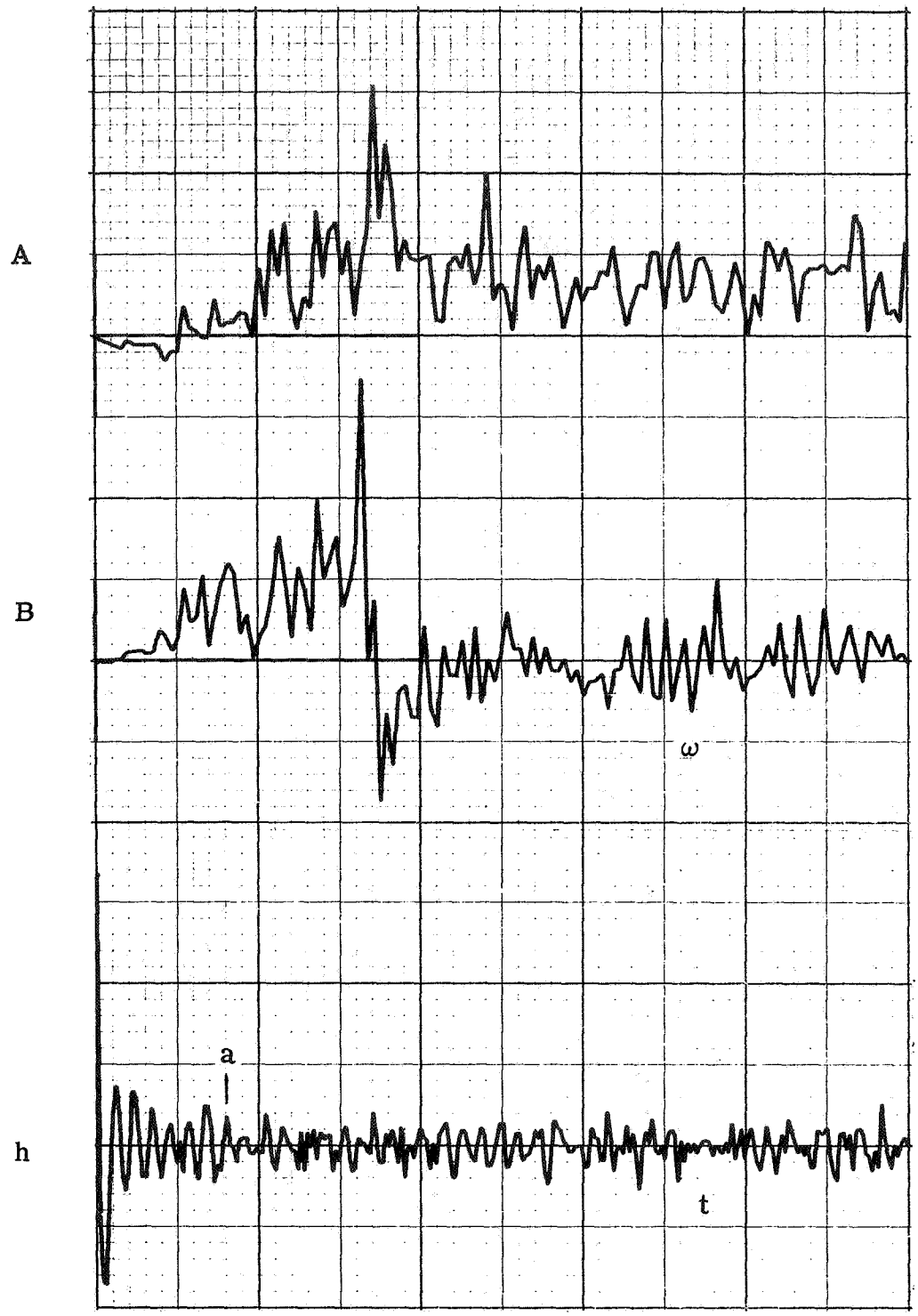

Figure 7.- Frequency response and h functions obtained by single swept sine run with noise in input.

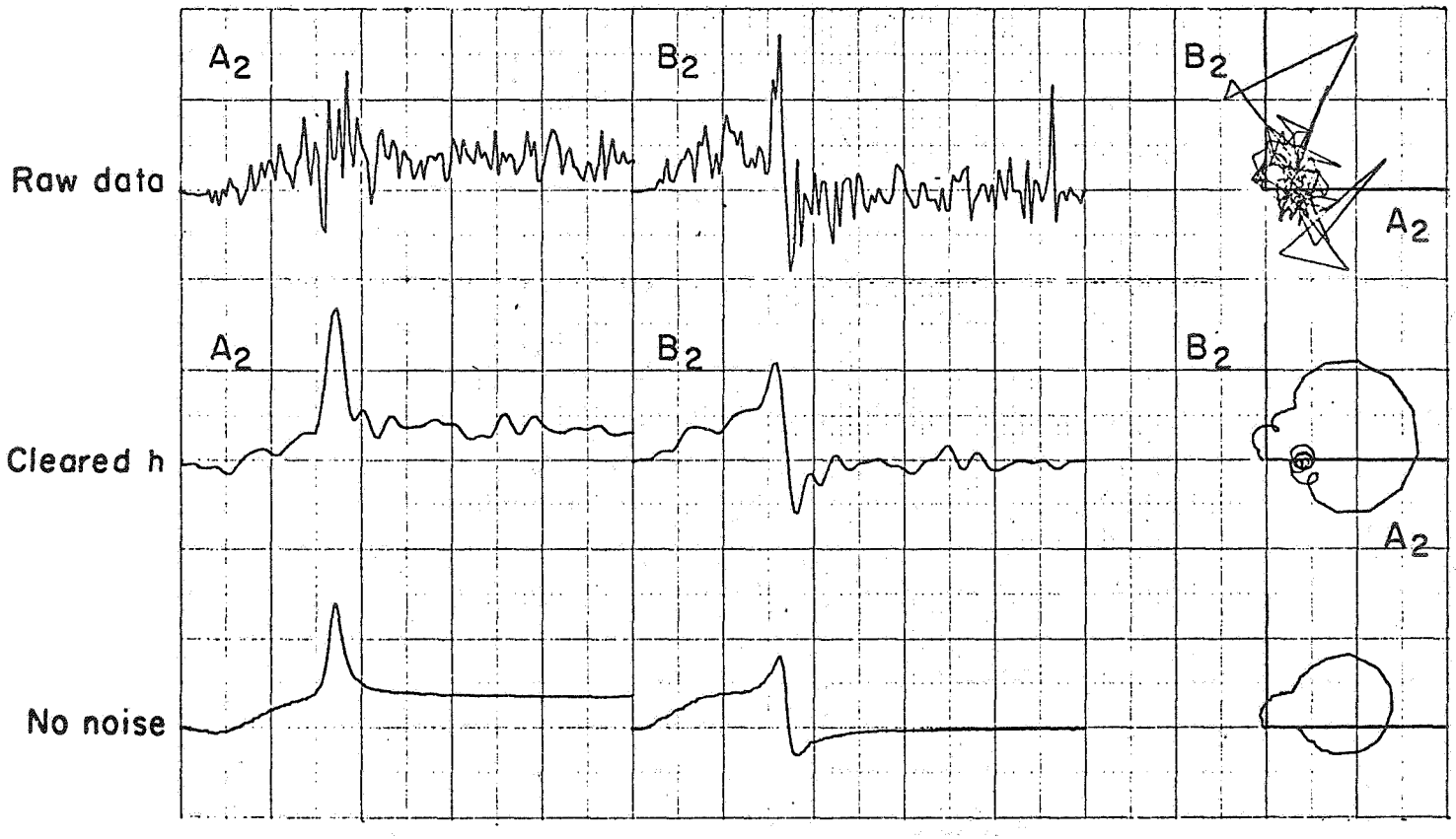

Figure 8.- Improved frequency response function by clearing h function.

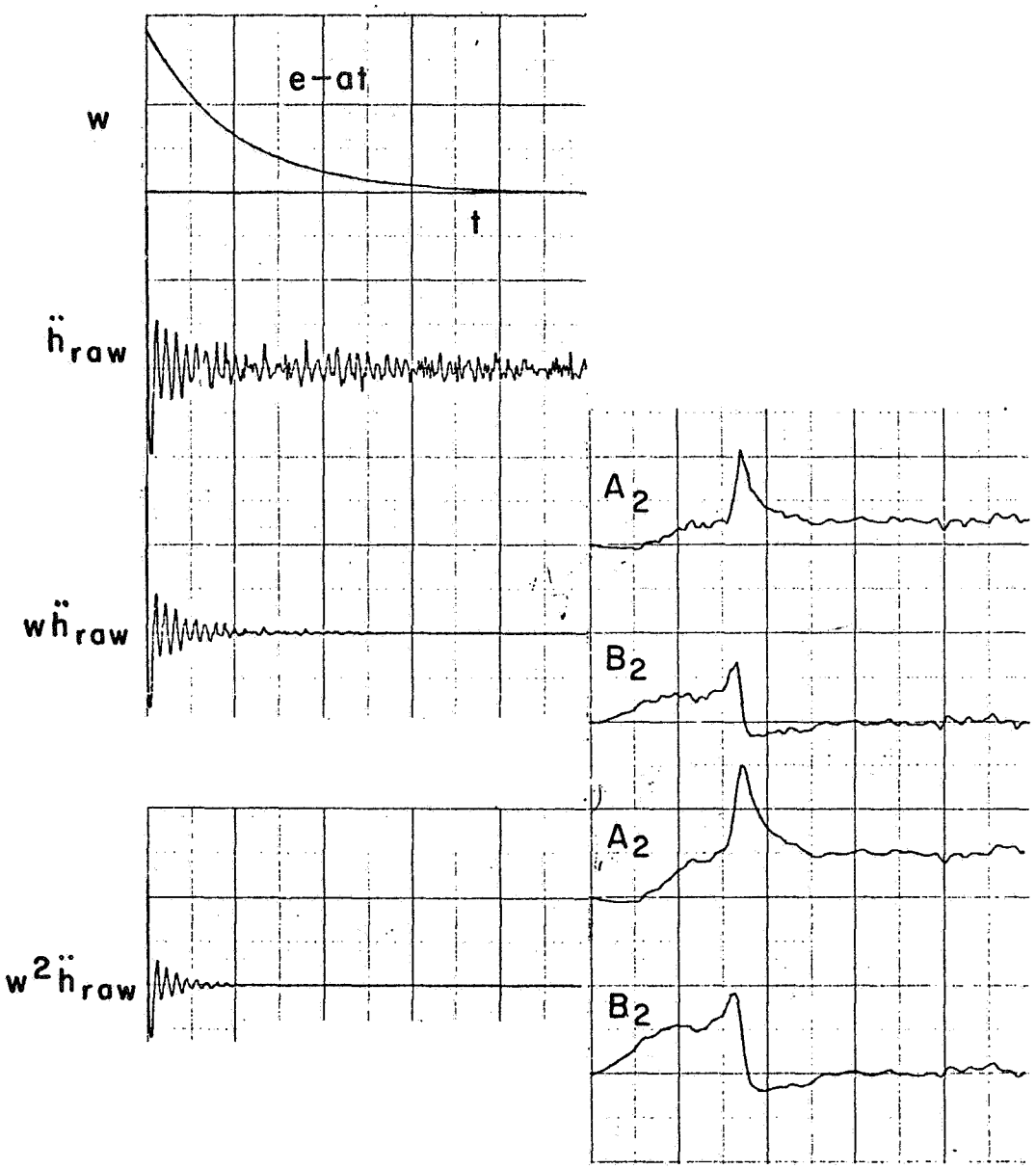

Figure 9.- Improved frequency response function by exponential weighting of h function.

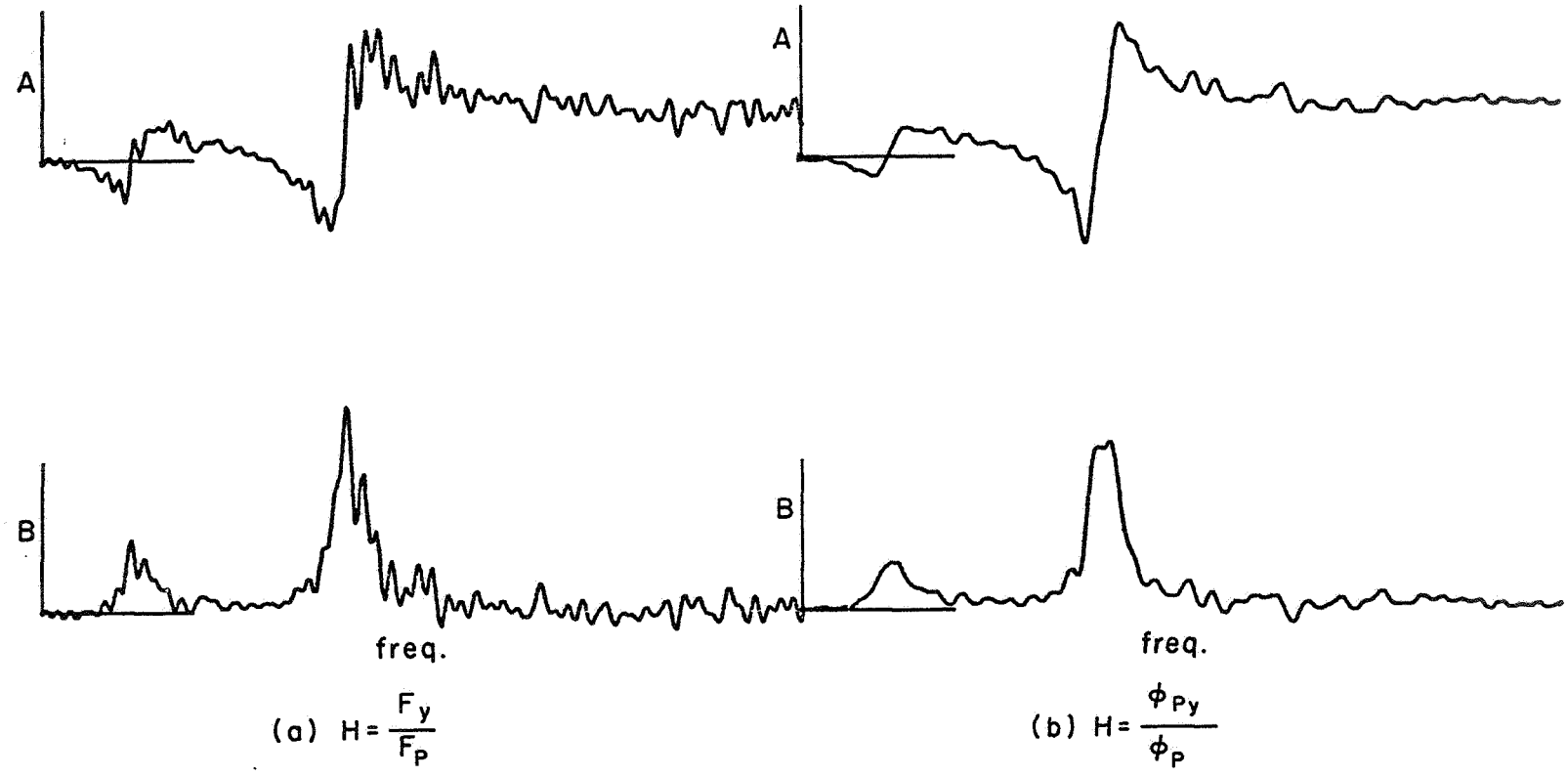

Figure 10.- Improvement in the deduction of H through use of cross-spectrum between input and output.

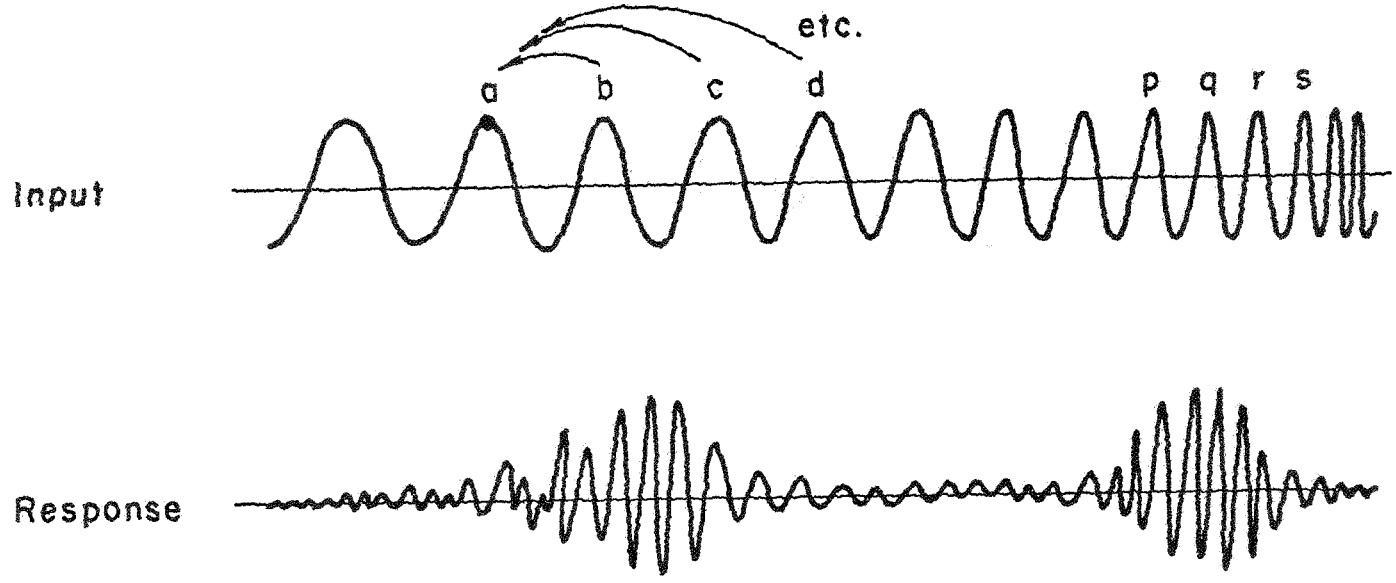

Figure 11.- Peak shifting to minimize noise effects.

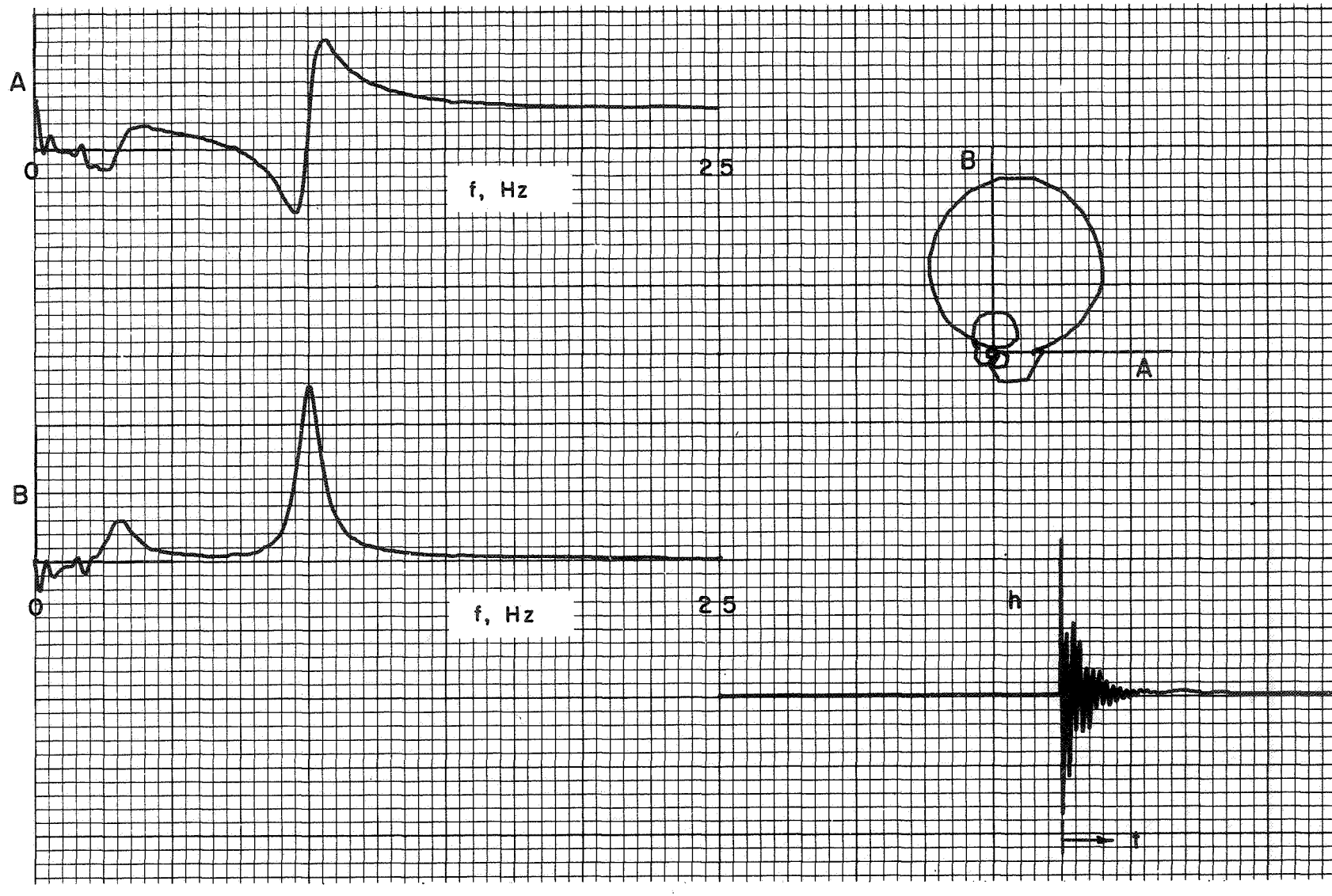

Figure 12.- Results obtained by peak shifting technique (19 shifts); original results very contaminated by noise.

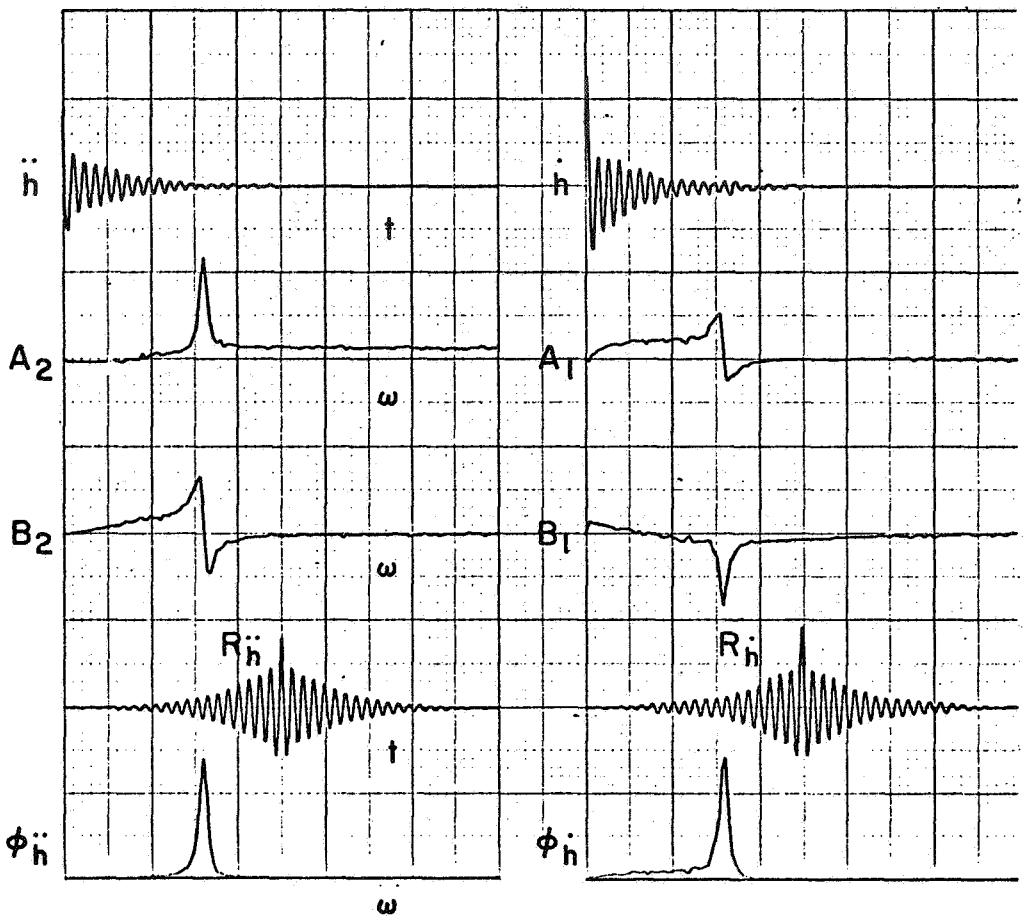

Figure 13.- Use of ensemble averaging of sine sweep runs to eliminate noise.

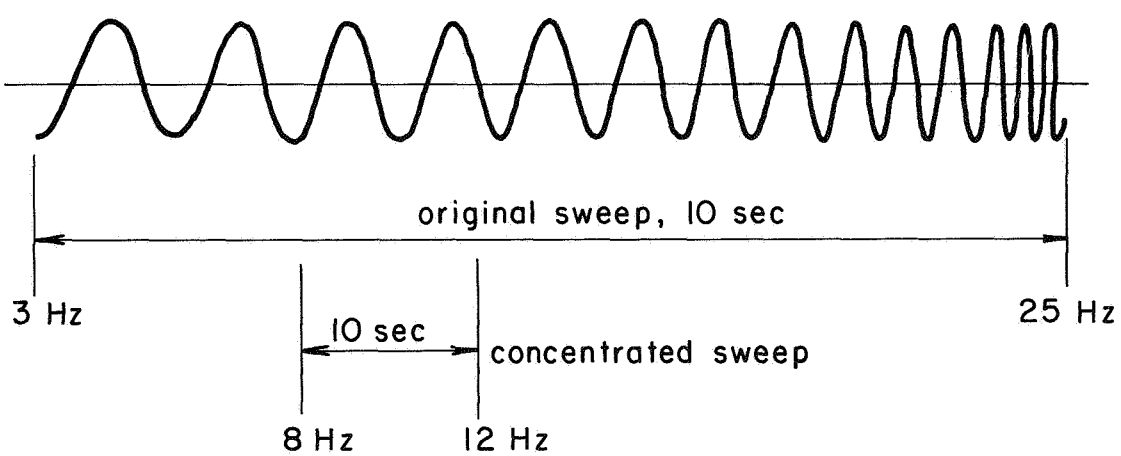

Figure 14.- Use of sweep over narrow frequency band.

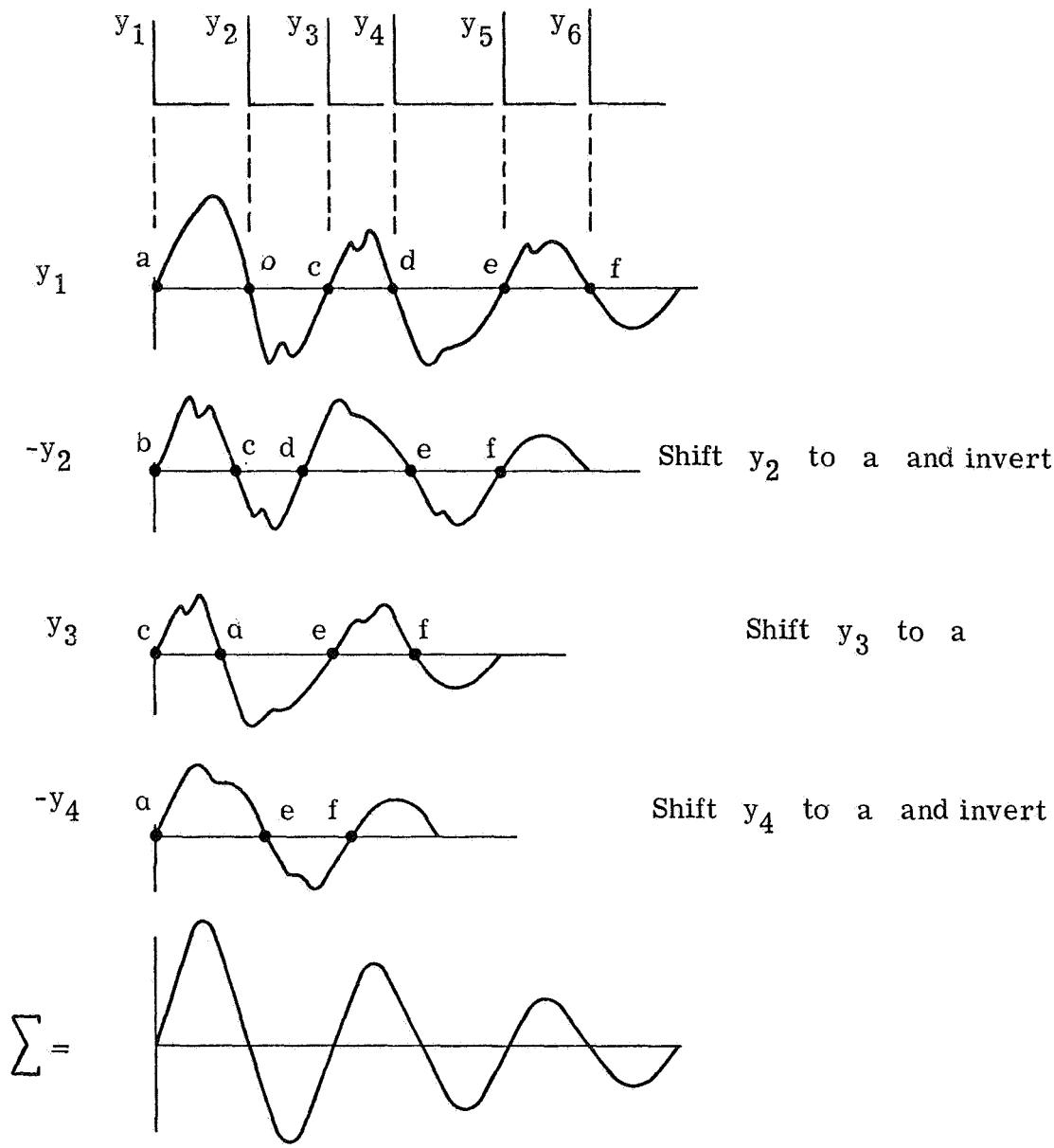

Figure 15.- "Randomdec" process to derive h-type function.

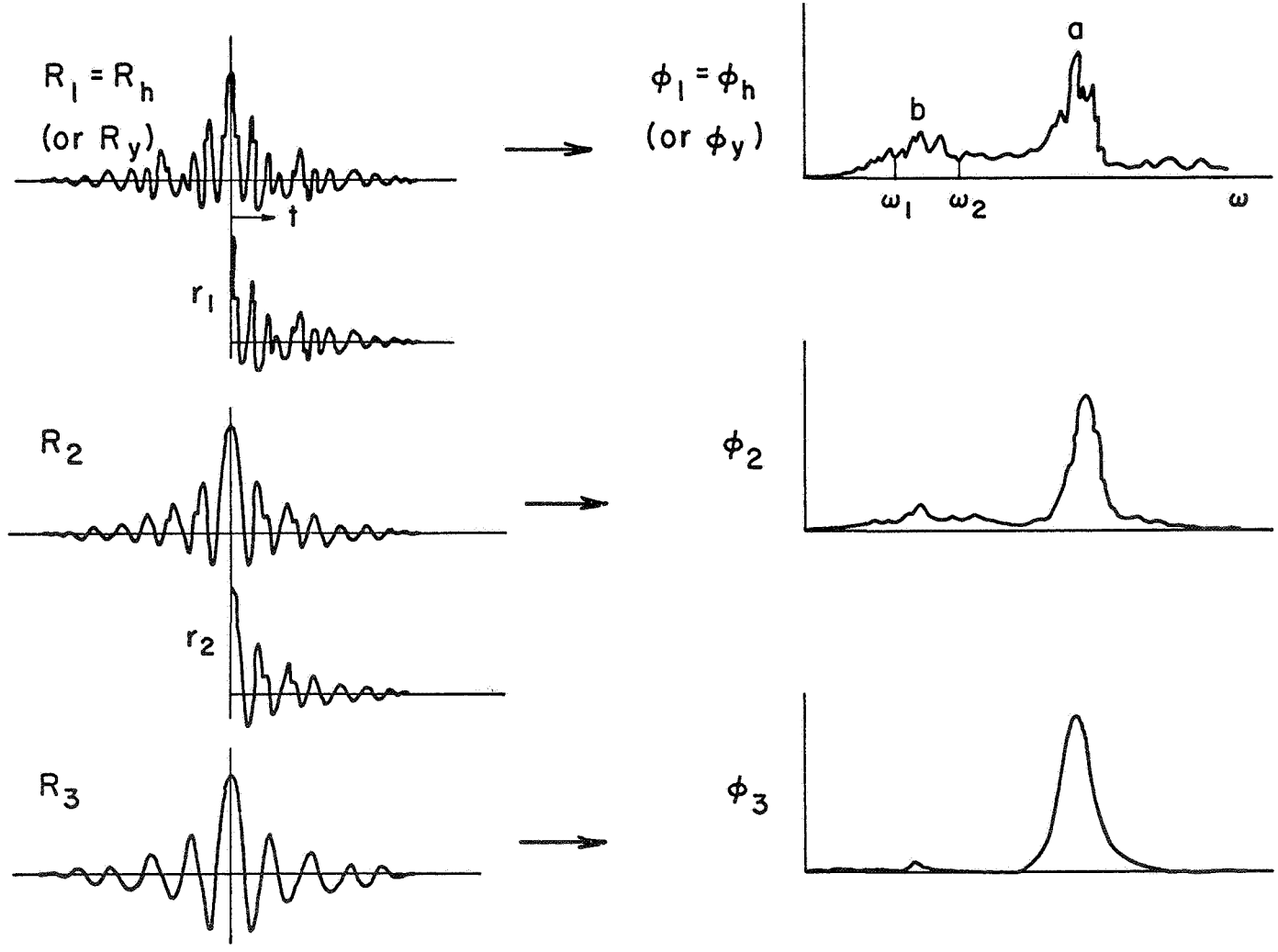

Figure 16.- Successive autocorrelations of one-sided correlation functions.

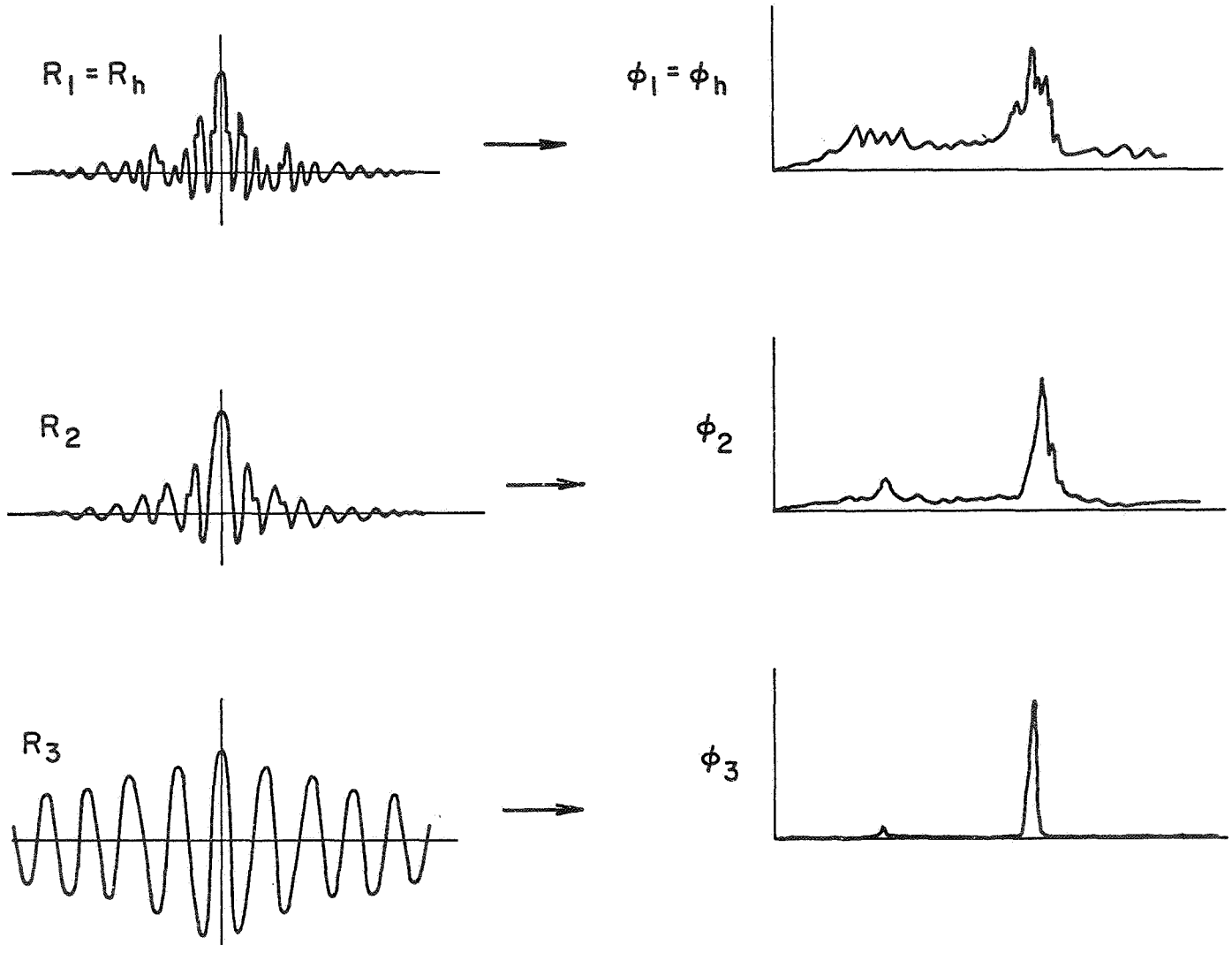

Figure 17.- Successive autocorrelations of two-sided correlation functions.

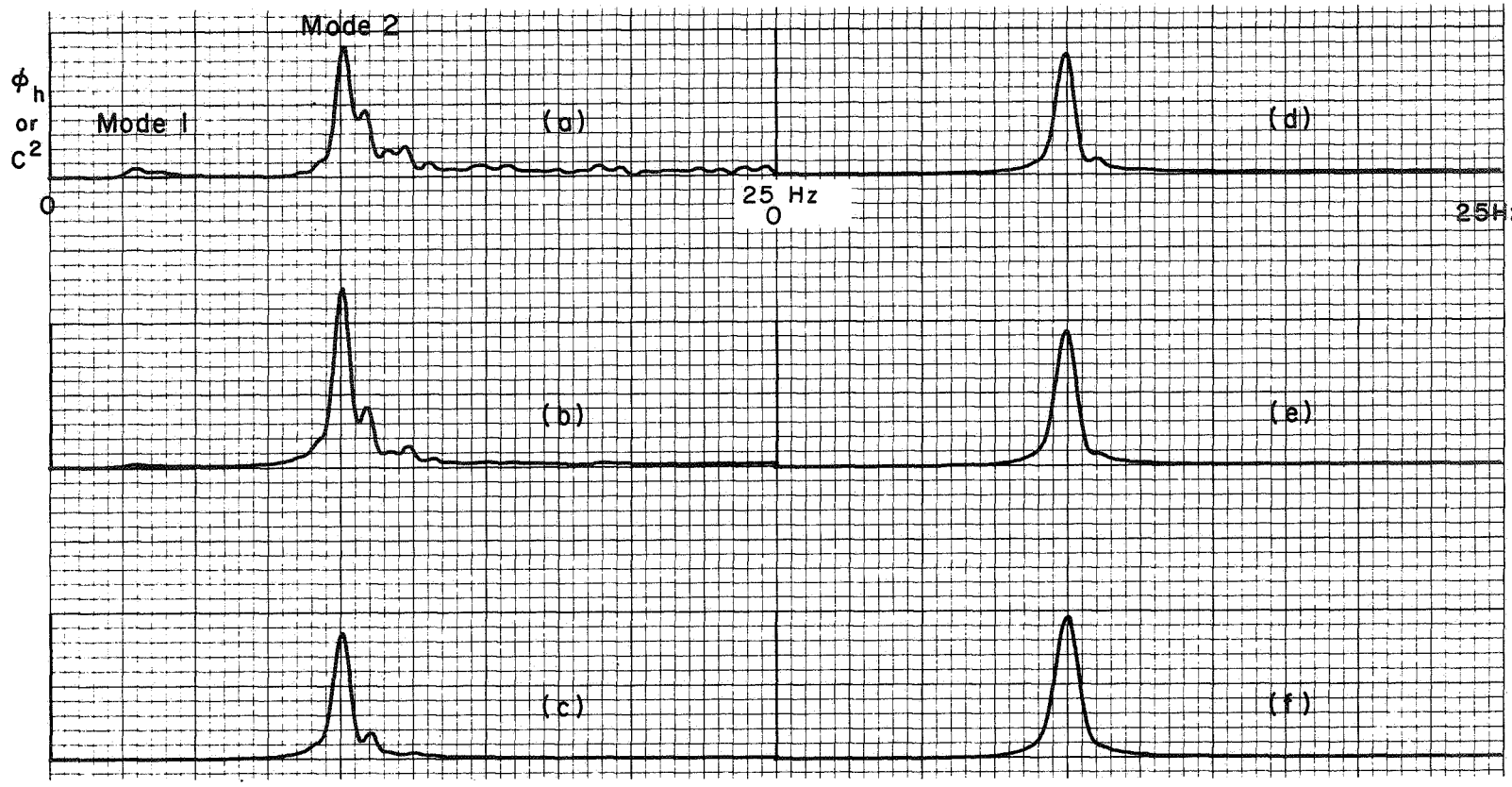

Figure 18.- Results obtained by successive correlations of one-sided correlation functions, starting with h as determined from raw H.

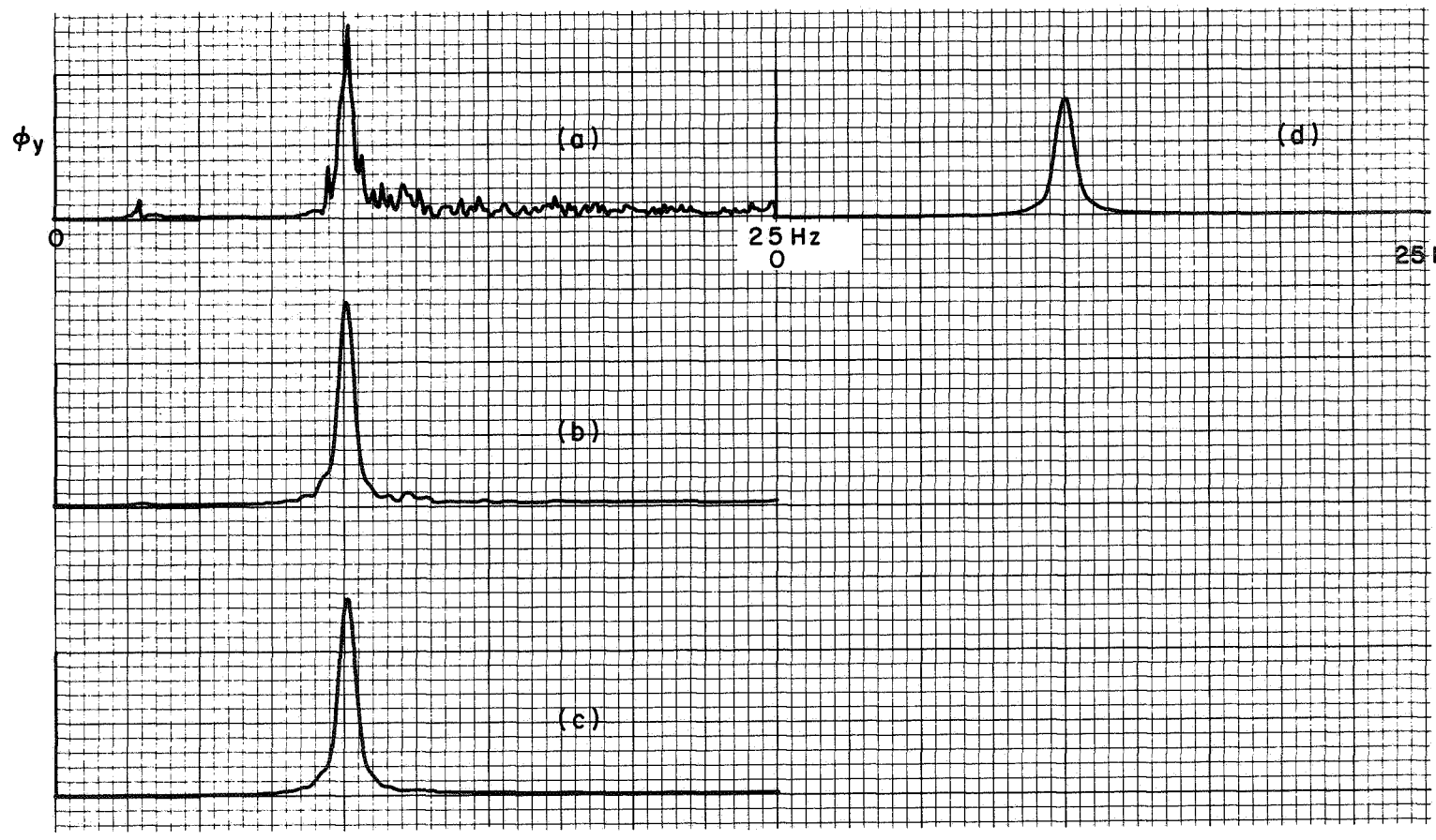

Figure 19.- Results obtained by successive correlations of one-sided correlation function, starting with R_y of the response only.

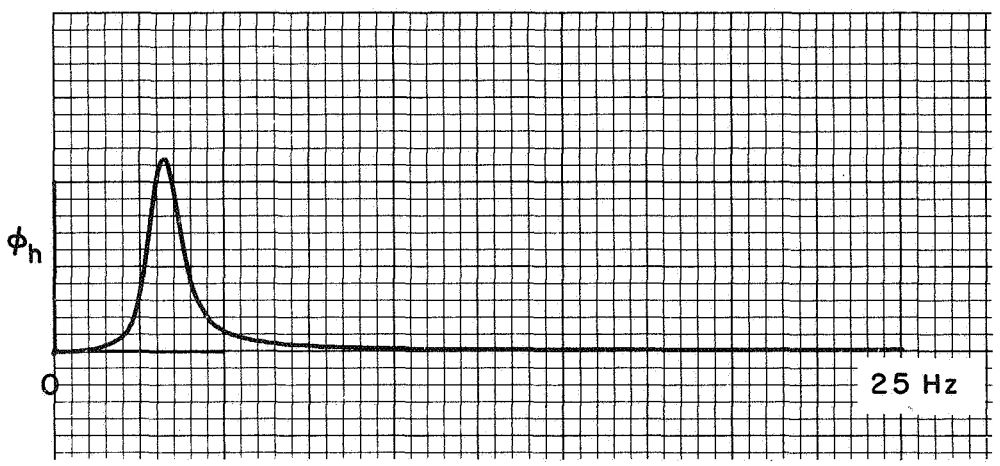

Figure 20.- Pure results for the low-frequency mode obtained by successive correlations of the one-sided correlation function.

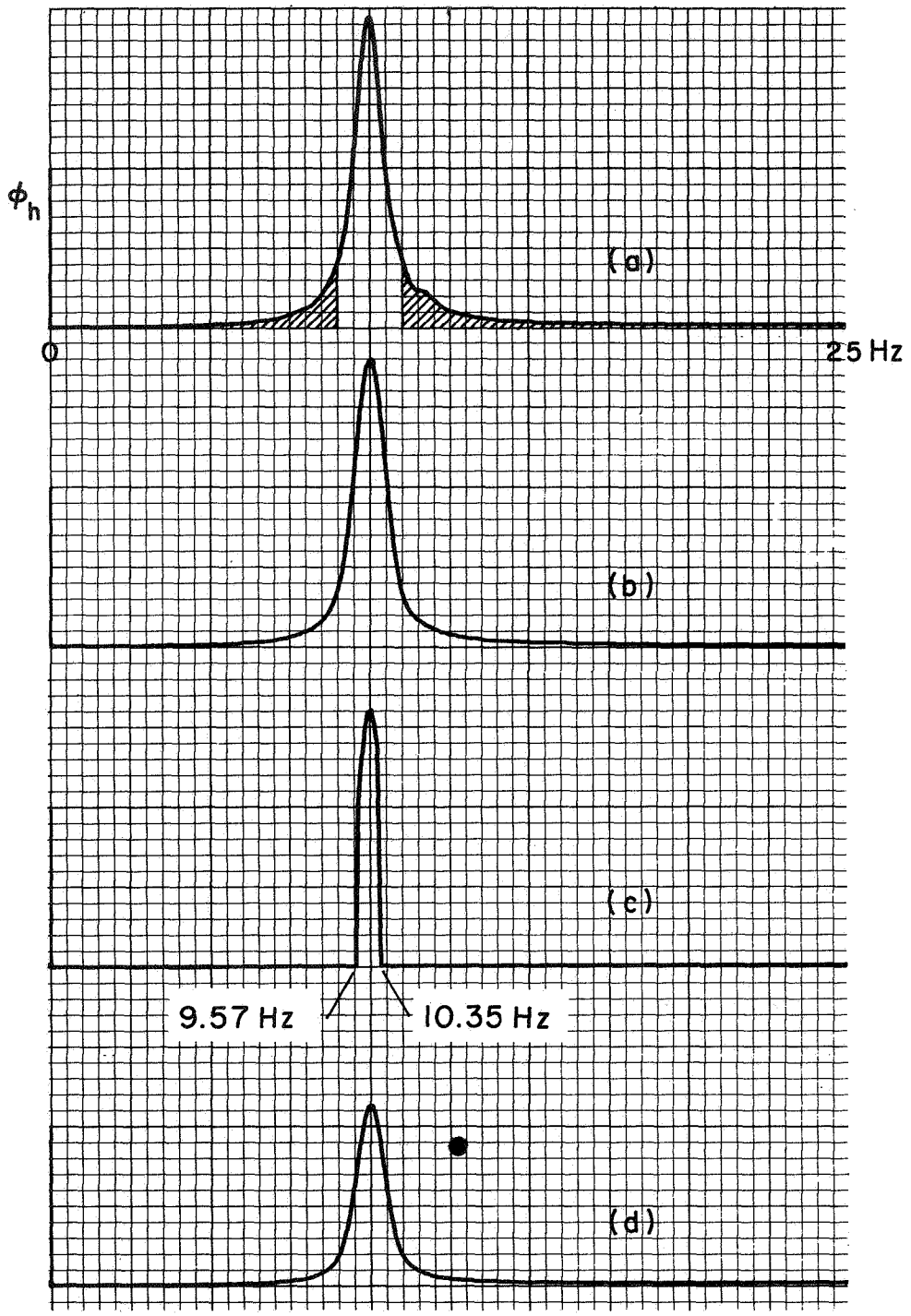

Figure 21.- Regeneration of modal response characteristics after truncation in the frequency plane.

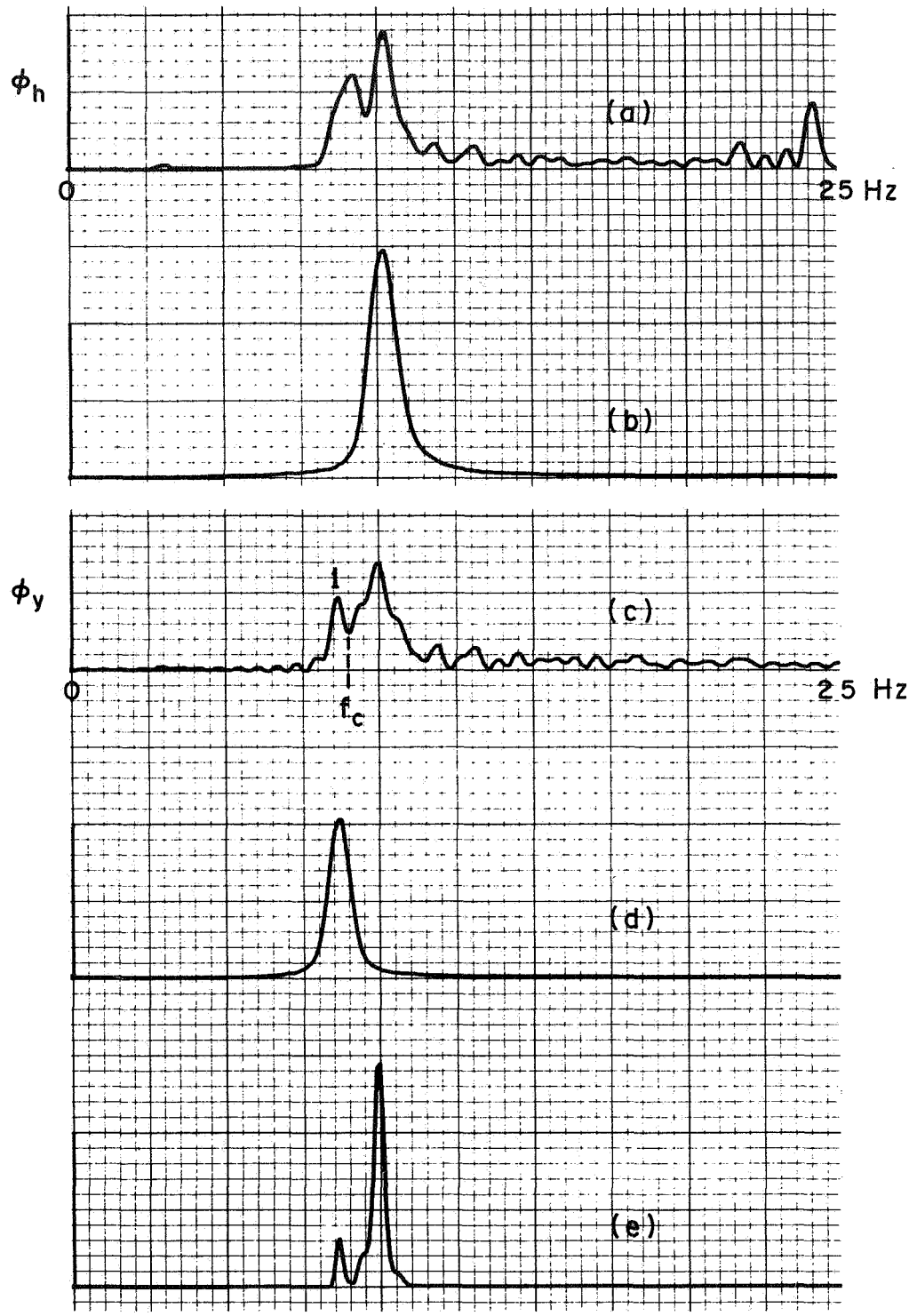

Figure 22.- Isolation of modes by frequency plane erasing, two-mode system.

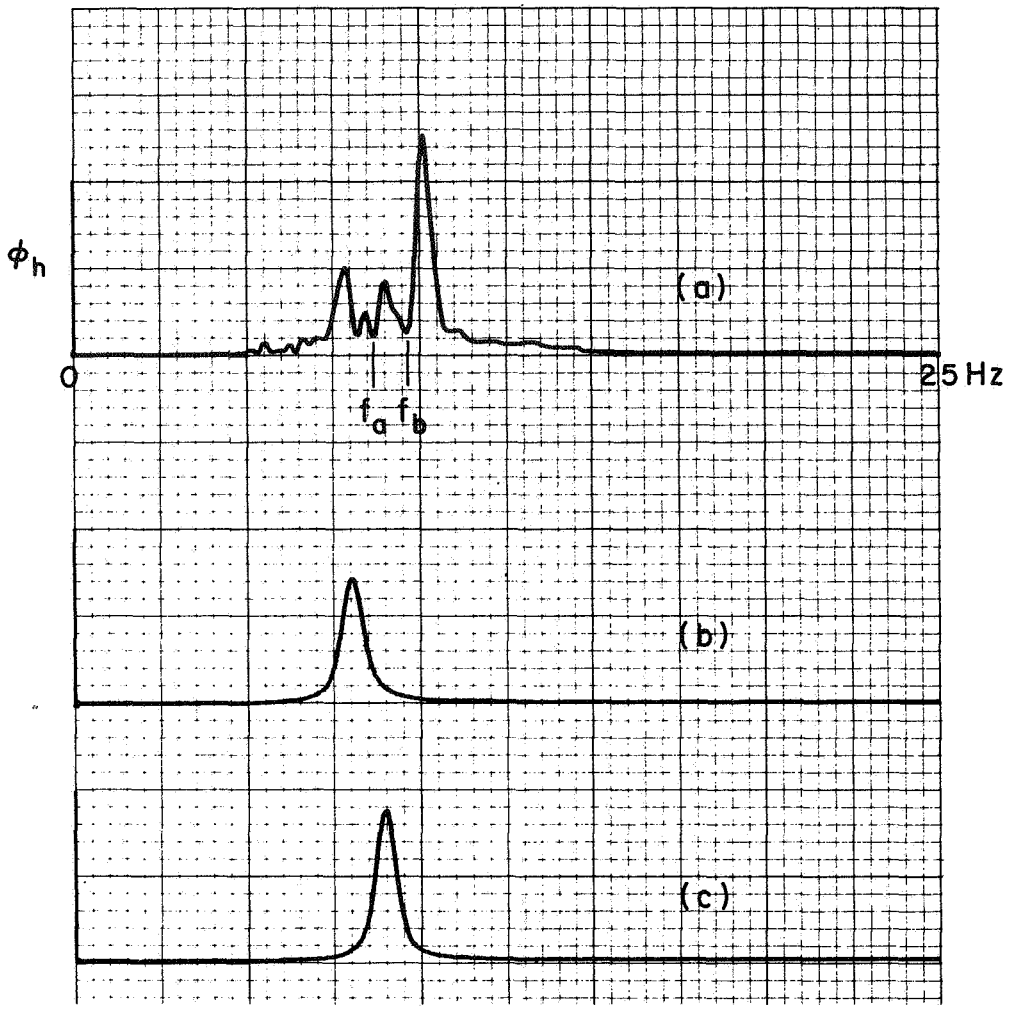

Figure 23.- Isolation of specific modes by frequency plane erasing, three-mode system.

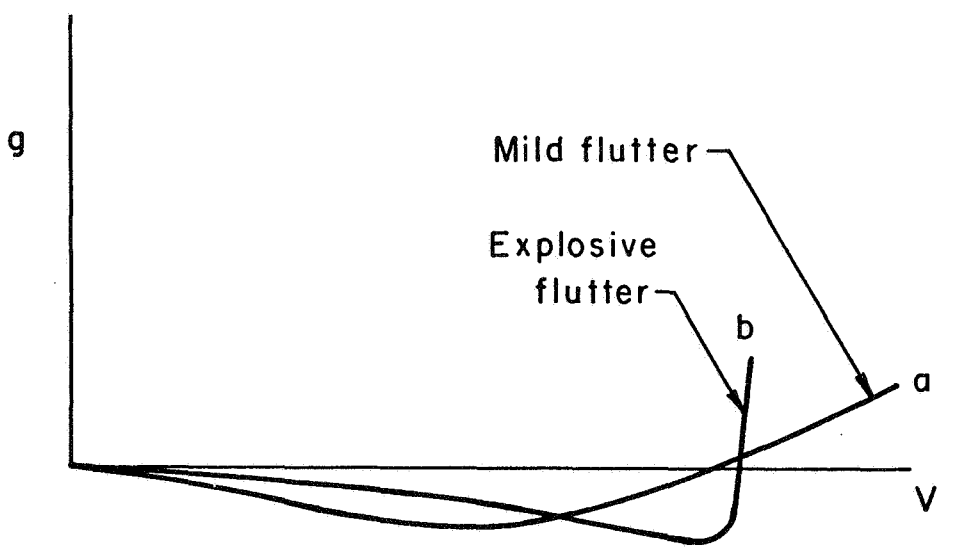

Figure 24.- Damping curves for mild and explosive flutter cases.

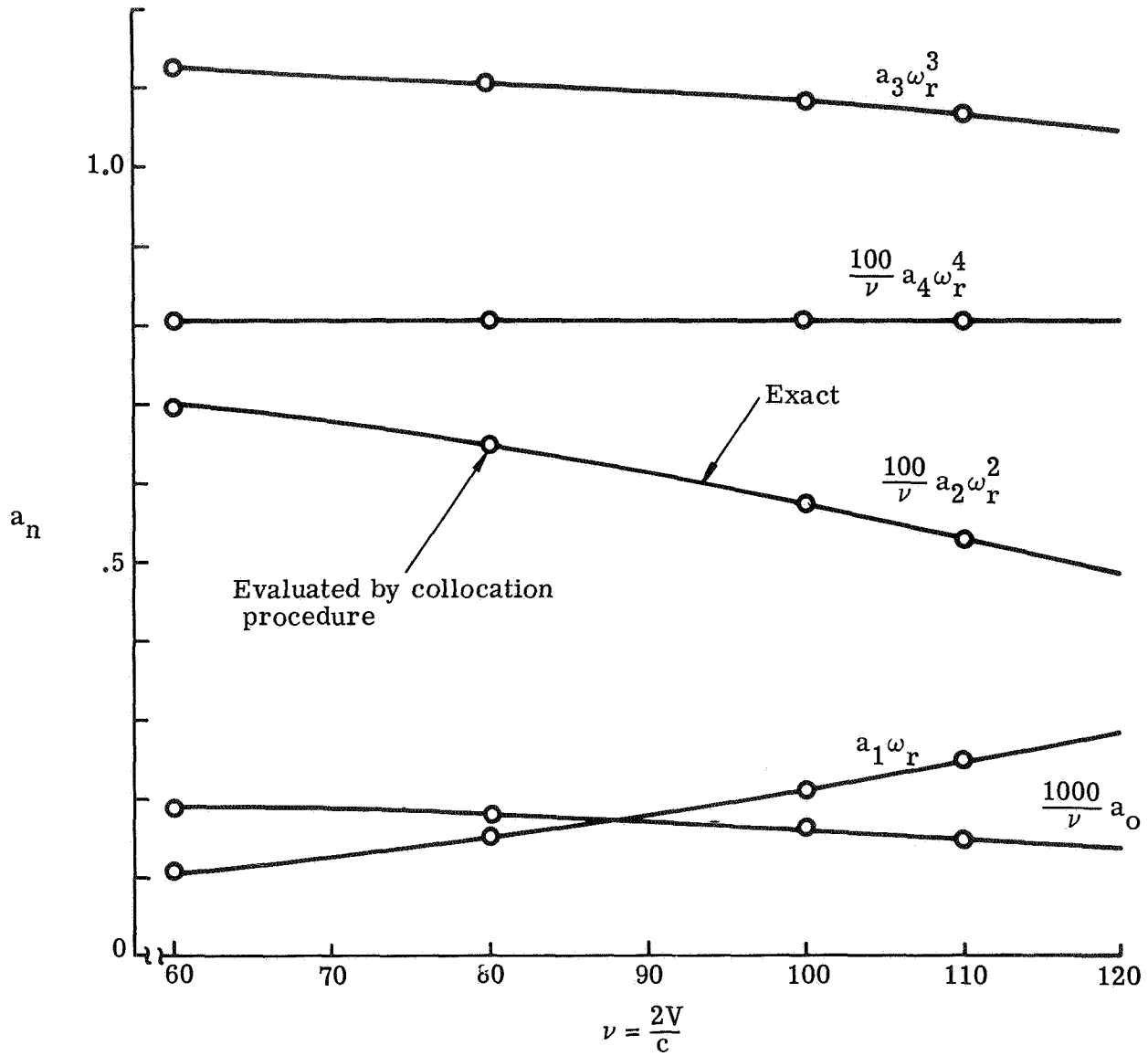

Figure 25.- Variation of differential equation coefficients with airspeed, mild flutter.

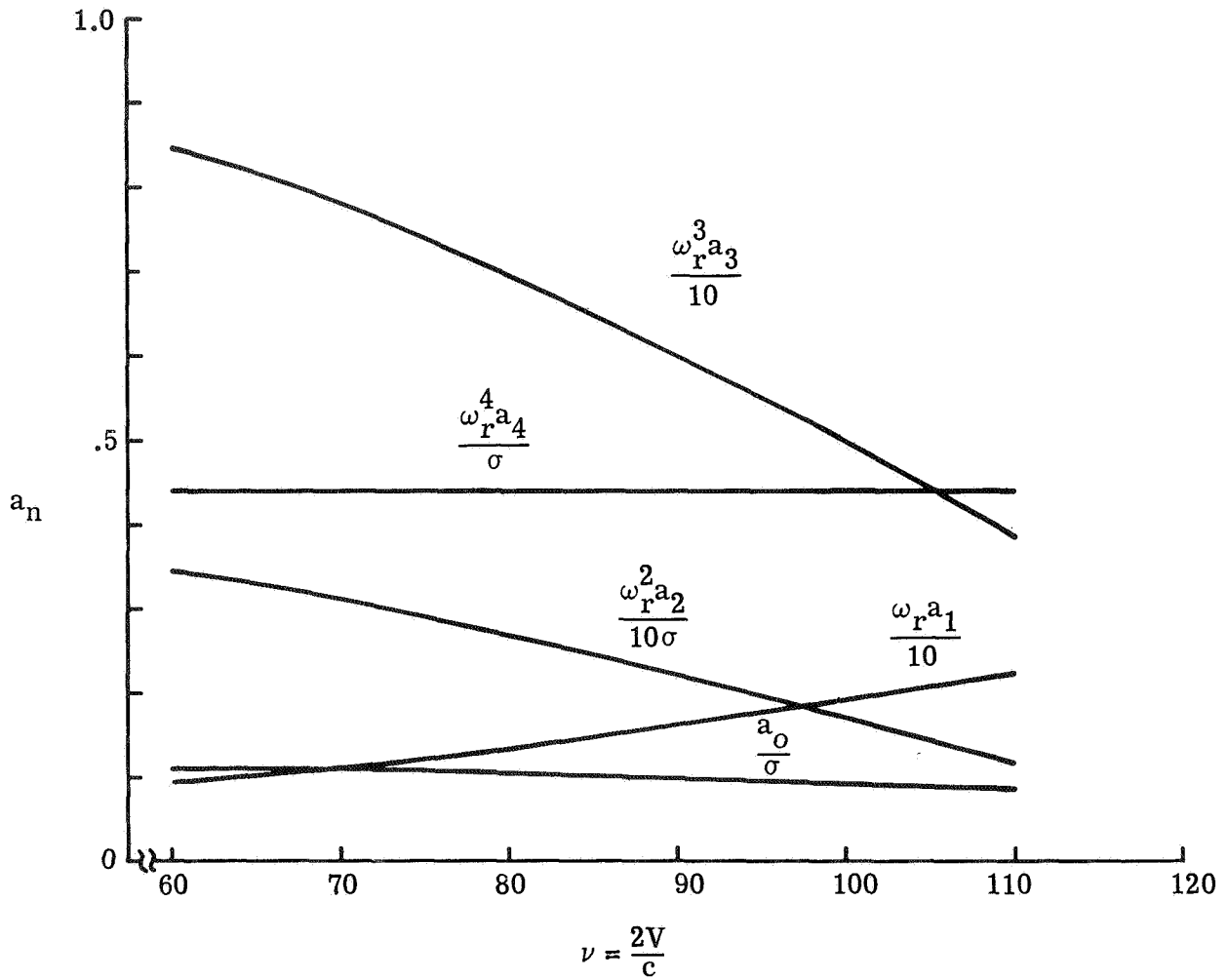

Figure 26.- Variation of differential equation coefficients with airspeed, explosive flutter.